# FIELD EVALUATION OF SENSORS FOR PRECIPITATION TYPE DISCRIMINATION

Wiel Wauben, Tiemo Mathijssen and Corné Oudshoorn
Royal Netherlands Meteorological Institute (KNMI)
P.O. Box 201, 3730 AE De Bilt, The Netherlands
email: Wiel.Wauben@knmi.nl and Tiemo.Mathijssen@knmi.nl

**ABSTRACT**

The Royal Netherlands Meteorological Institute (KNMI) uses the Vaisala FD12P present weather sensor for the automated determination of visibility and of the type, intensity and duration of precipitation in its national meteorological observation network. Replacement of the FD12P is required in the near future due to discontinuation of support by the manufacturer. For this purpose, a field evaluation is conducted using several instruments, which have been selected in order to cover various techniques with respect to precipitation type discrimination. The instruments participating in this evaluation are the Vaisala FD12P, Vaisala PWD22, Biral VPF750, Biral SWS250, Campbell Scientific PWS100, Ott Parsivel$^2$ and Thies LPM. The Optical Scientific OWI432 & HIP100 is envisaged but not yet available for the test. Not all selected instruments measure visibility. To accommodate replacement of the FD12P, these capabilities could be fulfilled by considering 2 separate sensors. Because earlier research pointed to difficulties of the FD12P to the discrimination of precipitation type during winter conditions, a special focus is put on the differences between sensors in the performance of this aspect.

A reference for precipitation type is not available. The results of the selected sensors are compared against the precipitation type reported by the FD12P. The precipitation type reported by FD12P is not always correct, but the characteristics of the FD12P are well known at KNMI after years of operational use. The preliminary results indicate that some sensors perform better in the specific problem areas of the FD12P, but some new issues arise. The field evaluation of the sensors is not yet completed. The field test is ongoing and will include the next winter season. The analysis of the data also requires further refinement. No preferred sensor has been identified at this moment.

The paper also gives preliminary results of the evaluation of precipitation amount and intensity reported by the selected sensors versus the KNMI precipitation gauge; the visibility reported by the sensors versus a transmissometer; and of the temperature, which the sensor uses in the discrimination of the precipitation type, versus the operational air temperature of the automatic weather station.

## 1. INTRODUCTION

KNMI employs the Vaisala FD12P Present Weather Sensor (PWS) in the national meteorological observation network since 1997. The FD12P is an optical forward scatter sensor that is capable of measuring visibility (Meteorological Optical Range, MOR) and for aeronautical applications the background luminance. In combination with the information obtained with a precipitation detector and a temperature sensor it also determines the type and intensity of precipitation. Since November 2002 all synoptic and climatological observations of KNMI are performed fully automatically (Wauben, 2002), in which the FD12P is used for the automated determination of MOR and present and past weather. More recently also the aeronautical observations have been automated with the exception of Amsterdam Airport Schiphol. In this case, the FD12P provides the aeronautical visibility, Runway Visual Range (RVR) and present and recent weather. In all situations the instantaneous 1-minute averaged MOR, background luminance and precipitation intensity and -type of the FD12P are used. KNMI algorithms convert the sensor information into information that is reported to the users. Currently, KNMI uses FD12P sensors at 4 civil airports, 8 military airbases, 13 North sea platforms and 12 automatic weather stations for the fully automated generation of synoptic, climatological and aeronautical reports. Although the FD12P sensor serves KNMI well, there have been issues related to the calibration of the MOR (Bloemink, 2006) and the reduction of MOR due to flying insects (Wauben, 2012). The discrimination of precipitation type of the FD12P also remains an area with room for improvement (De Haij and Wauben, 2010; Wauben, 2014).

KNMI employs approximately 75 FD12P sensors. The FD12P is out of production since the middle of 2010 and the manufacturer support of the sensor will end in 2019. Hence, KNMI needs a successor of the FD12P. In the evaluation presented in this paper, the focus will be on the discrimination of precipitation type. The evaluation of sensors reporting precipitation type is difficult and no reference exist. Therefore KNMI selected and purchased several present weather sensors in order to get experience with these sensors and to be of help in the preparations for the upcoming specification and evaluation that will be part of an European tender. Although some of the selected sensors have been tested before by other institutes, these evaluations generally did not include more than half of the selected sensors. Also the conditions during these tests are not comparable to those in The Netherlands, where for example solid or mixed precipitation around 0 °C is crucial.

## 2. SELECTED PRESENT WEATHER SENSORS AND FIELD SETUP

The FD12P present weather sensor needs not necessarily be replaced by a single sensor, but separate sensors for visibility and for precipitation type and intensity will also be considered. The field evaluation for precipitation type discrimination includes the following sensors:

- Vaisala FD12P present weather sensor (firmware 1.92S). The FD12P is currently used operationally by KNMI. All other sensors will be compared against this sensor. The FD12P does not serve as the reference, but the characteristics and the strong and weak points of the FD12P are known by KNMI.
- Vaisala PWD22 present weather detector (firmware 2.07). The successor of the FD12P is the FS11P, but the precipitation type and intensity information of this sensor is obtained with a PWD22 sensor. The PWD22 uses the same measurement principle as the FD12P. It consists of a forward scatter sensor, where spikes in the optical signal indicate the size of precipitation particles, and a precipitation detector gives information on the liquid water content. The PWD22 is equipped with a temperature sensor that is also used in the precipitation type discrimination. The PWD22 measures MOR up to 20 km.
- Biral SWS250 present weather sensor (firmware SI100245.06A). The SWS250 is a forward scatter and backscatter sensor that determines the precipitation type from the size-velocity distribution of the particles and the ratio of forward- to backscatter. The size and velocity of the particles is determined from the magnitude and the duration of the spikes in the scattered signal. The SWS250 is equipped with a temperature sensor that is also used in the precipitation type discrimination. The SWS250 is the latest in the line of new compact present weather sensors of Biral. The SWS250 measures MOR up to 75 km.
- Biral VPF750 present weather sensor (firmware 245.04.02.3). The VPF750 uses the same measurement principle as the SWS250. The VPF750 is of the older line of present weather sensors of Biral, but it is considered the most capable present weather sensor available from Biral in that it reports the greatest number of present weather types or codes and uses a temperature and humidity sensor to detect freezing precipitation. Since KNMI uses its own operational temperature and humidity sensors for the discrimination of freezing precipitation and has its own algorithms to generate the present, recent and past weather codes the SWS250 is a suitable choice. The Biral VPF750 is included in the test because it was already available at the test site of KNMI in De Bilt. The VPF750 measures MOR up to 75 km.
- Thies LPM laser precipitation monitor (firmware V2.53). The LPM is a disdrometer that produces a horizontal light beam and measures its intensity. When a particle falls through the light beam the signal is reduced. The amplitude of the reduction determines the size and the duration of the reduced signal gives the fall speed of the particle. The precipitation type is determined form the size-velocity distribution. The LPM is equipped with a temperature sensor to improve the precipitation type identification. Two LPM instruments were already available at the test site from a previous test. Both have been upgraded to the latest version. Visibility is not measured by the LPM.
- Ott Parsivel$^2$ present weather sensor (firmware 2.02.5, in August the firmware was upgraded to 2.10.1). The Parsivel$^2$ is a disdrometer that uses the same measurement principle as the LPM. The Parsivel$^2$ is not equipped with a temperature sensor for improving precipitation type identification. A

Parsivel was already available at the test site from a previous test. It could not be upgraded, so it was replaced by the Parsivel$^2$. Visibility is not measured by the Parsivel$^2$.

- Campbell Scientific PWS100 present weather sensor (firmware 007628-07). The measurement technique of the PWS100 is a combination of a disdrometer and a forward scatter sensor. The transmitter produces four evenly spaced horizontal light sheets that are parallel to each other. Two receivers measure the scattered radiation at equal angles in the horizontal and in the vertical plane. The fall speed of the particle is determined from the time interval between the peaks as it passes the light sheets and the delay between the peaks detected by the horizontal compared to the vertical detector gives the size. The sensor determines the precipitation type from the size and velocity measurements and the structure of the received signal. The PWS100 is equipped with a temperature and humidity sensor to enhance precipitation type discrimination. The PWS100 measures MOR up to 20 km.
- Optical Scientific OWI430&HIPS weather identifier and visibility sensor. The OWI430 is a combination of a forward scatter and a scintillation sensor, which determines the precipitation type and intensity from the precipitation induced scintillation. The OWI430 can be equipped with an acoustic HIP sensor for the discrimination of hail and ice pellets. The OWI430 measures MOR up to 10 km.

**Table 1: Overview of the requirements and specifications of the selected present weather sensors.**

| Sensor | Visibility | Background luminance | Precipitation intensity | Precipitation duration | Precipitation type |
|---|---|---|---|---|---|
| WMO / ICAO | MOR 10 m – 100 km<br>VIS 10 m – 10 km<br>1 m<br>± 50 m ≤ 600 m<br>± 10% @ 600 – 1500 m<br>± 20% > 1500 m<br>RVR 10 – 2000 m<br>± 10 m ≤ 400 m<br>± 25 m @ 400 – 800 m<br>± 10% > 800 m<br>achievable<br>maximum of 20 m or 20% | 0 – 40000 cd/m$^2$<br>1 cd/m$^2$<br>± 10 % | 0.02 – 2000 mm/h<br>0.1 mm/h<br>detection @ 0.02 – 0.2 mm/h<br>± 0.1 mm/h @ 0.2 – 2 mm/h<br>± 5 % > 2 mm/h | Threshold >0.02 mm/h<br>1 minute<br>± | 8 types<br>& UP & FZ & mixtures<br>UP, DZ, RA, SN, PL, SG, IC, GS, GR<br><br>ps. IC for WMO only |
| Vaisala<br>FD12P & LM21 | 10 m – 50 km<br>1 m<br>± 10 % @ 10 m – 10 km<br>± 20 % @ 10 – 50 km | 2 – 40000 cd/m$^2$<br>1 cd/m$^2$<br>± 10 % | 0.00 – 999.99 mm/h<br>0.01 mm/h<br>± 30 % @ 0.5 – 20 mm/h liquid | ≤0.05 mm/h in 10’ | 8 types<br>& UP & FZ & mixtures<br>UP, (FZ)DZ, (FZ)RA, SN, PL, SG, IC, GS, GR |
| Vaisala<br>PWD22 & PWL111 | 10 m – 20 km<br>1 m<br>± 10 % @ 10 m – 10 km<br>± 15 % @ 10 – 20 km | 4 – 20000 cd/m$^2$<br>1 cd/m$^2$<br>? | 0.00 – 999.99 mm/h<br>0.01 mm/h<br>? | ≤0.05 mm/h in 10’ | 4 types<br>& UP & FZ & mixtures<br>UP, (FZ)DZ, (FZ)RA, SN, PL |
| Biral<br>VPF-750 & ALS-2 | 10 m – 75 km<br><br>≤2 % @ 600 m – 2 km<br>≤11 % @ 30 km | 2 – 40000 cd/m$^2$<br>1 cd/m$^2$<br>≤10 % | 0.015 – ~500 mm/h<br><br>≤10 % | 0.00025 mm/min =<br>0.015 mm/h liquid<br>0.0015 mm/h snow<br>Ø <0.2 – >3.2 mm #21<br>0.4 – >20 m/s #16 | 7 types<br>& UP & FZ & mixtures<br>UP, (FZ)DZ, (FZ)RA, SN, PL, SG, IC, GR |
| Biral<br>SWS-250 & ALS-2 | <10 m – 2 km (75km)<br>10 m<br>≤5 % < 2 km<br><10 % @ ~10 km<br><15 % @ ~20 km<br><20 % @ ~30 km | 2 – 40000 cd/m$^2$<br>1 cd/m$^2$<br>≤10 % | 0.015 – ~500 mm/h<br><br>≤15 % | 0.00025 mm/min =<br>0.015 mm/h liquid<br>0.0015 mm/h snow | 7 types<br>& UP & mixtures<br>UP, DZ, RA, SN, IP, SG, IC, GS/GR |
| Campbell Scientific<br>PWS100 | 0 m – 20 km<br><br>± 10 % @ 0 m – 10 km | 0 – 45000 cd/m$^2$<br>0.1 cd/m$^2$<br>± 0.5 ≤ 5 cd/m$^2$<br>± 10 % > 5 cd/m$^2$ | 0.00 – 400 mm/h<br><br>± 10 % typically | 0.0001 mm/h<br>Ø 0.1 – 30 mm #34<br>0.16 – 30 m/s #34 | 8 types<br>& UP & FZ & mixtures<br>UP, (FZ)DZ, (FZ)RA, SN, PL, SG, IC, GS, GR |
| Ott<br>Parsivel$^2$ | - | - | 0.001 – 1200 mm/h<br>0.001 mm/h<br>± 5 % liquid<br>± 20 % solid | Ø 0.2 – 5 mm, #32<br>25 mm solid<br>0.2 – 20 m/s, #32 | 6 types<br>& mixtures<br>DZ, RA, SN, PL, SG, GR |
| Thies | - | - | <0.005 – >1000 mm/h | Ø 0.16 – > 8 mm, #22 | 6 types |

| Sensor | Visibility | Background luminance | Precipitation intensity | Precipitation duration | Precipitation type |
|---|---|---|---|---|---|
| LPM | | | 0.001 mm/h<br>≤15 % @ 0.5 – 20 mm/h liquid<br>≤30 % snow | 0.2 – > 10 m/s, #20 | & UP & FZ & mixtures<br>UP, (FZ)DZ, (FZ)RA, SN, PL/GS, SG/IC, GR |
| Optical Scientific OWI430 & HIPS | 1 m – 30 km<br><br>± 10 % @ 1 m – 5 km<br>± 15 % @ 5 – 10+ km | 0 – 10000 cd/m$^2$<br><br>± 5 % | 0.1 – 3000 mm/h<br><br>± 5 % liquid<br>± 10 % snow | 0.1 mm/h liquid<br>0.01 mm/h snow<br>0.001 mm accumulation | 5 types<br>& UP & FZ & mixtures<br>UP, (FZ)DZ, (FZ)RA, SN, PL, GR |

An overview of the requirements and the specifications of the selected present weather sensors is given in Table 1. Reported are the range, resolution and measurement uncertainty of the meteorological units reported by the sensors. Since the focus in this study is on precipitation type discrimination, the visibility range of the selected sensors was not optimized. Sometimes sensors with a limited visibility range have been selected although versions were available with a larger range. The background luminance sensor is also not purchased for this evaluation. Note that the selected present weather sensors cover a variety of measurement techniques. Techniques that are not included are Doppler radar systems, 2D video disdrometers or dedicated hail or freezing precipitation sensors. The reasons for not including sensors applying these techniques varies. They are either too expensive, not ready for operational 24*7 use, cannot be considered as a replacement for the FD12P, or were considered to be not as promising as the selected sensors.

The selected sensors were purchased and directly installed in the test field at the main premises of KNMI in De Bilt. The sensors have not been subjected to laboratory tests since they are difficult to perform and the results with respect to precipitation type discrimination are limited. The focus was on getting the sensors in the field as fast as possible in order to make optimal use of the winter period. The sensors were installed at existing locations on the test field around the middle of February 2016. Only the OWI430&HIPS has not yet been obtained due to KNMI difficulties with procurement procedures. Figure 1 shows the setup of the selected present weather sensors on the test field in De Bilt. The test field is also equipped with a standard Automatic Weather Station (AWS) so that meteorological information of for example air temperature, humidity and wind is available. A Vaisala Mitras transmissometer is available on the test field and serves as the reference for MOR values up to 2 km. A rain gauge of in-house design serves as the reference for the precipitation amount and intensity reported by the selected present weather sensors. For high visibility values and for precipitation type, no reference is available, but the selected present weather sensors will be compared against the results obtained with the FD12P since the characteristics and the strong and weak points of the FD12P are known by KNMI after years of operational use. In addition, the precipitation type will be evaluated using camera images of the test field and by considering the meteorological conditions. The 1-minute averaged values (or shorter) of the meteorological units of all present weather sensors under evaluation have been acquired with an update interval of at least 1 minute. When possible, raw data from which the precipitation type has been derived has also been archived. This facilitates more detailed analysis and future optimization and reprocessing by the manufacturer. The evaluation period considered in this paper is from February 18, 2016 to July 31, 2016.

For the evaluation 1-minute sensor data is used. For precipitation type the “maximum” or most important type according to the order in Table 2 in the previous minute is considered. For precipitation intensity, MOR and temperature 1-minute averages are considered. Note that one or more valid sensor values in the preceding minute leads to a valid 1-minute value. No processing has been performed to the sensor data. Sensor data is used as reported. Hence a correction of the precipitation type, such as discrimination of freezing/non-freezing using the operational air temperature sensor in a radiation screen, is not performed.

An overview of the results for precipitation type, precipitation intensity, MOR and temperature is given in sections 3, 4, 5 and 6, respectively. Section 7 gives some examples of illustrative results by showing the PWS measurements on selected days. A reader with an interest in precipitation type only can skip sections 4 to 6. However, it should be noted that precipitation intensity is relevant for precipitation type because an intensity threshold is used for reporting precipitation type. Also the precipitation type eventually needs to be reported in intensity classes. The temperature of the PWS is also relevant since it is used by the PWS (with the exception of Parsivel[2]) in the precipitation type discrimination. This can partially be done off-line, for example to determine whether liquid precipitation is freezing or non-freezing, but sometimes information is not available off-line, for example to determine the type when snow is reported at a too high temperature. The relevancy of MOR for precipitation type is that precipitation affects the MOR. Situations can occur that are meteorologically inconsistent, for example when dense drizzle or heavy snow is reported but there is no visibility reduction. Also dense fog or visibility reductions caused by flying insects, can sometimes trigger precipitation. In these cases the MOR should also be considered in the evaluation of the precipitation type.

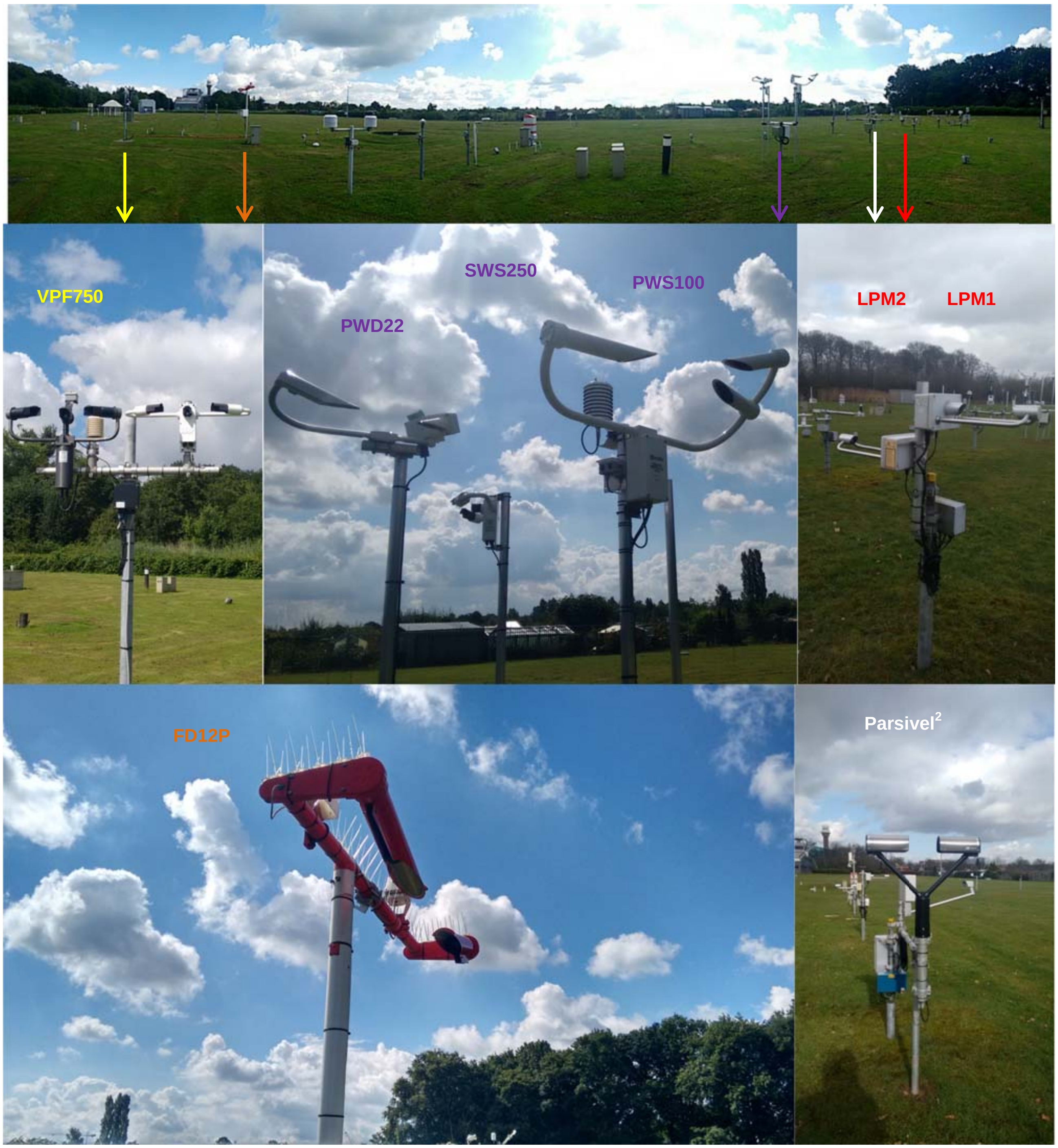


**Figure 1: Overview of the selected present weather sensors under evaluation at the test field of KNMI in De Bilt.**

## 3. GENERAL OVERVIEW OF THE RESULTS FOR PRECIPITATION TYPE

In this section an overview of the results for the 1-minute precipitation type reported by the PWSs under evaluation is given. The instantaneous precipitation type is reported by the sensor in the so-called NWS code of the National Weather Service, the METAR weather code of ICAO or the wawa weather code of WMO. Note that here only the codes concerning precipitation type at the moment of observation are considered. Other codes are treated as no precipitation. In terms of the NWS code the following cases can be distinguished: "C" means clear or no precipitation; "P" for unidentified precipitation; "L" for drizzle; "ZL" for freezing drizzle; "LR" for a mixture of drizzle and rain; ZL" for freezing drizzle; "R" for rain; "ZR" for freezing rain; "RS" for a mixture of rain and snow; "S" for snow; "IP" for ice pellets; "SG" for snow grains; "IC" for ice crystals; "SP" for snow pellets; and "A" for hail. The precipitation type can also be divided in the classes: unidentified precipitation (P); liquid precipitation (L, LR or R); freezing precipitation (ZL or ZR); and solid precipitation (RS, S, IP, SG, IC, SP or A); or most generally in terms of precipitation (all types). Detection of precipitation is in fact considered in the last case. The relation between NWS and wawa code and between NWS and METAR code is given in Figure 2.

The relative occurrence of the precipitation types reported by all present weather sensors in the evaluation period is given in Table 2. Here the row indicated by "NA" gives the percentage of 1-minute intervals in the evaluation period with unavailable data or when the sensor reported an invalid precipitation type. About 0.2 to 6.1 % of the data is unavailable. Data is mostly missing due to problems with the network and data-acquisition. The Parsivel$^2$ sometimes stopped operating and did not respond to the polling command anymore and had to be restarted to resume the data-acquisition. The line indicated by "C" denotes the percentage of valid cases that the sensor reported that there was no precipitation, whereas "precipitation" gives the percentage of valid cases that the sensor reported any type of precipitation. Precipitation is reported 9 to 10 % of the time by the two Vaisala sensors and the Pasivel2. The two Biral sensors report precipitation less often (about 6.5 %) whereas the PWS100 and LPM report precipitation more often (about 13 to 14 %). This indicates that the PWS100 and LPM are more sensitive and the VPF750 and SWS250 less sensitive compared to the FD12P. The KNMI precipitation gauge reported precipitation 9 % of the time during the evaluation period. Note that the above results apply when no intensity threshold is used for reporting precipitation and precipitation type, whereas WMO recommends using a threshold of > 0.02 mm/h for reporting precipitation. Note that KNMI experiences generally no problems with the FD12P regarding precipitation detection. KNMI uses the FD12P in combination with a 0.05 mm/h reporting threshold for synoptic purposes, and 0.03 mm/h for aeronautical purposes.

The next rows of Table 2 give the percentage of time that precipitation is reported as a specific type ("P" to "A") or class ("unidentified" to "solid"). Here only the 1-minute intervals when a sensor reports precipitation are considered. Hence the sum of all types and the sum of all classes add up to 100 % for each sensor. The FD12P is 3% of the time unable to identify the type of precipitation, for the PWS100 this is nearly 10 % and for the LPM it is the case for 2 to 4 % of the precipitation events. The other sensors do not report any cases with unidentified precipitation. The results for the LPM are surprising since previous field evaluations showed that the LPM generally reports unidentified precipitation as a result of spiders or spider webs. Note that unidentified precipitation is not a desirable result since users have to assume the worst precipitation type. However, generally unidentified precipitation is overruled by any other precipitation type that occurs in the interval that is used for reporting the weather in the synoptic and aeronautical reports. Liquid precipitation has been reported most often by all sensors and ranges between 89 % (for PWS100) and 98 %. Liquid precipitation occurs mainly as rain. The rain to drizzle ratio varies widely between the sensors and is largest for the PWD22 (83:15) and VPF750 (77:20) and smallest for the Parsivel$^2$ (42:56). The LPM is the only sensor that reports a mixture of rain and drizzle as the instantaneous precipitation type. The deviations in the rain and drizzle classification suggest that there are discrepancies in the estimation of the size of the detected precipitation particles. This will be investigated in more detail in the next section when precipitation intensity is considered.

The occurrence of freezing precipitation is negligible and is only reported by the FD12P and the VFP750. Note that the discrimination of freezing or liquid precipitation by the sensor is not relevant for KNMI as freezing or non-freezing precipitation will be determined by the operational temperature sensor of KNMI. Precipitation occurs approximately 2 % of the time as solid precipitation. The VPF750 and SWS250 reported more solid precipitation (3 and 6 %, respectively) and the PWS100 less (1 %), but the latter reports many unidentified precipitation events. The experience with the FD12P is that it generally reports too few solid precipitation events, particularly when the temperature is around zero degrees and in situations with wet snow. Solid precipitation is recorded mostly as snow by all sensors, except for the VPF750 and SWS250, where the mixture of rain and snow dominates. Also note the relatively high values of SG reported by the FD12P (a known problem that occurs during dense fog) and by the VPF750 and SWS250; IP reported by the PWD22; and SP reported by the Parsivel[2].

**Table 2: The relative occurrence of the 1-minute precipitation type reported by the selected present weather sensors during the evaluation period.**

| NWS | wawa | FD12P | PWD22 | VPF750 | SWS250 | PWS100 | Parsivel[2] | LPM1 | LPM2 |
|---|---|---|---|---|---|---|---|---|---|
| NA | - | 0.281% | 0.239% | 4.607% | 0.764% | 0.848% | 6.131% | 2.068% | 2.090% |
| C | 0 | 89.958% | 90.398% | 93.363% | 93.525% | 87.070% | 90.838% | 86.019% | 86.560% |
| precipitation | >0 | 10.042% | 9.602% | 6.637% | 6.475% | 12.930% | 9.162% | 13.981% | 13.440% |
| P | 40 | 3.022% | 0.000% | 0.000% | 0.000% | 9.875% | 0.000% | 4.211% | 1.785% |
| L | 50 | 36.401% | 14.504% | 20.043% | 30.141% | 22.596% | 55.894% | 33.290% | 33.623% |
| ZL | 55 | 0.042% | 0.000% | 0.386% | 0.000% | 0.000% | 0.000% | 0.000% | 0.000% |
| LR | 57 | 0.000% | 0.000% | 0.000% | 0.000% | 0.000% | 0.000% | 13.476% | 13.647% |
| R | 60 | 58.353% | 83.119% | 76.541% | 64.357% | 66.767% | 41.786% | 47.461% | 49.256% |
| ZR | 65 | 0.000% | 0.000% | 0.000% | 0.000% | 0.000% | 0.000% | 0.000% | 0.000% |
| RS | 67 | 0.483% | 0.000% | 1.609% | 3.177% | 0.000% | 0.088% | 0.372% | 0.422% |
| S | 70 | 1.026% | 1.837% | 0.379% | 0.838% | 0.735% | 1.072% | 0.876% | 0.908% |
| IP | 75 | 0.092% | 0.540% | 0.000% | 0.000% | 0.003% | 0.000% | 0.181% | 0.221% |
| SG | 77 | 0.559% | 0.000% | 0.452% | 1.192% | 0.023% | 0.000% | 0.031% | 0.048% |
| IC | 78 | 0.000% | 0.000% | 0.000% | 0.000% | 0.000% | 0.000% | 0.000% | 0.000% |
| SP | 87 | 0.000% | 0.000% | 0.186% | 0.131% | 0.000% | 0.974% | 0.000% | 0.000% |
| A | 89 | 0.021% | 0.000% | 0.406% | 0.164% | 0.000% | 0.186% | 0.101% | 0.090% |
| unidentified | | 3.022% | 0.000% | 0.000% | 0.000% | 9.875% | 0.000% | 4.211% | 1.785% |
| liquid | | 94.755% | 97.623% | 96.583% | 94.498% | 89.363% | 97.680% | 94.227% | 96.527% |
| freezing | | 0.042% | 0.000% | 0.386% | 0.000% | 0.000% | 0.000% | 0.000% | 0.000% |
| solid | | 2.181% | 2.377% | 3.031% | 5.502% | 0.762% | 2.320% | 1.562% | 1.689% |

A suitable method to compare the precipitation type reported by the different sensors is by means of a contingency matrix. The contingency matrix shows the number of times a specific type is reported by a sensor (row) and the type reported by the “reference” sensor (column) at that moment. The contingency matrix for the PWD22 versus the FD12P is given in Figure 2. It indicates the wawa code in second row and second column, but also the corresponding NWS and METAR codes in the first row and column, respectively. The numbers given in the contingency matrix can be used to calculated scores for each individual precipitation type. However, this is not always suitable since not all types are reported by each sensor. Furthermore, the number of cases involved for some types is small and the distinction between some types, even between drizzle and rain, is not always relevant for users. Hence it is more suitable to calculate the scores for the precipitation classes. The classes are indicated by the boxes in Figure 2. The vertical blocks indicate cases when no precipitation (white); unidentified precipitation (grey); liquid precipitation (blue); freezing precipitation (orange) and solid precipitation (green) is reported by the “reference” sensor. The solid colours indicate cases where both sensors report the same precipitation class. Note that the order of the precipitation types in Figure 2 has been changed compared to Table 2 in order to facilitate the indication of the precipitation classes.

| PWD22 \ FD12P | | C | P | L | LR | R | ZL | ZR | RS | S | IP | SG | IC | SP | A |
|---|---|---|---|---|---|---|---|---|---|---|---|---|---|---|---|
| | | 0 | 40 | 50 | 57 | 60 | 55 | 65 | 67 | 70 | 75 | 77 | 78 | 87 | 89 |
| GR | 89 | 0 | 0 | 0 | 0 | 0 | 0 | 0 | 0 | 0 | 0 | 0 | 0 | 0 | 0 |
| GS | 87 | 0 | 0 | 0 | 0 | 0 | 0 | 0 | 0 | 0 | 0 | 0 | 0 | 0 | 0 |
| IC | 78 | 0 | 0 | 0 | 0 | 0 | 0 | 0 | 0 | 0 | 0 | 0 | 0 | 0 | 0 |
| SG | 77 | 0 | 0 | 0 | 0 | 0 | 0 | 0 | 0 | 0 | 0 | 0 | 0 | 0 | 0 |
| PL | 75 | 6 | 7 | 0 | 0 | 80 | 0 | 0 | 16 | 14 | 0 | 0 | 0 | 0 | 0 |
| SN | 70 | 2 | 5 | 0 | 0 | 74 | 0 | 0 | 75 | 210 | 22 | 30 | 0 | 0 | 0 |
| RASN | 67 | 0 | 0 | 0 | 0 | 0 | 0 | 0 | 0 | 0 | 0 | 0 | 0 | 0 | 0 |
| FZRA | 65 | 0 | 0 | 0 | 0 | 0 | 0 | 0 | 0 | 0 | 0 | 0 | 0 | 0 | 0 |
| FZDZ | 55 | 0 | 0 | 0 | 0 | 0 | 0 | 0 | 0 | 0 | 0 | 0 | 0 | 0 | 0 |
| RA | 60 | 983 | 308 | 5241 | 0 | 12226 | 10 | 0 | 24 | 3 | 0 | 4 | 0 | 0 | 5 |
| DZRA | 57 | 0 | 0 | 0 | 0 | 0 | 0 | 0 | 0 | 0 | 0 | 0 | 0 | 0 | 0 |
| DZ | 50 | 309 | 125 | 2390 | 0 | 477 | 0 | 0 | 0 | 0 | 0 | 0 | 0 | 0 | 0 |
| UP | 40 | 0 | 0 | 0 | 0 | 0 | 0 | 0 | 0 | 0 | 0 | 0 | 0 | 0 | 0 |
| | 0 | 211726 | 274 | 1030 | 0 | 1016 | 0 | 0 | 0 | 17 | 0 | 99 | 0 | 0 | 0 |

**Figure 2: Contingency matrix of the 1-minute precipitation types reported by the PWD 22 versus the FD12P present weather sensor during the evaluation period.**

The numbers given in the contingency matrix can be used to calculated some statistical quantities that give information about the measure of agreement between data sets of the two sensors under consideration. The quantities are the slope of the linear regression, the standard error of the linear fit and the correlation coefficient of the 1-minute precipitation type reported by a sensor versus the type reported by the FD12P. The values for these quantities are given in Table 3 and shown in Figure 3 for all PW sensors. The PWD22 shows generally the best agreement with the FD12P. The PWS100 and LPM show good results for the slope, whereas the VPF750 and SWS250 perform good for the standard error. The results for the correlation coefficient show the same trend as the slope, but the results for the PWD22 exceed that of the other sensors more clearly. Note that the calculation of these quantities includes situations with no precipitation, which occur most often. Other quantities that have been considered are the percentage of cases that no-precipitation and precipitation (denoted by “correct y&n”) are in agreement relative to the number that both sensors have valid data; the percentage of cases that the precipitation type (“correct type”) is in agreement relative to the number that both sensors report precipitation; and the percentage of cases that the precipitation class (“correct class”) is in agreement relative to the number that both sensors report precipitation. The latter two quantities are the fraction of cases with precipitation that are exactly on the diagonal of Figure 2 and the fraction in the solid coloured areas, respectively. These quantities also give some insight in the agreement between the sensors. The PWD22 compares again best with the FD12P in terms of “correct y&n”. Note that the KNMI precipitation gauge has a score of 95 % for “correct y&n”. In terms of “correct type”, the VFP750 and SWS250 compared best to the FD12P and the LPM the worst. In terms of “correct class” the SWS250 and PWS100 differ the most from the FD12P. The last 2 scores are mainly determined by the drizzle and rain events that occur most often. Lower scores for “correct type” indicate differences in type discrimination between drizzle and rain (or a mixture of drizzle and rain). When the classes are considered, these events all are in the liquid class and the scores improve.

**Table 3: Overview of several quantities indicating the agreement between the 1-minute precipitation type reported by a PWS and the FD12P during the evaluation period.**

| Quantity | PWD22 | VPF750 | SWS250 | PWS100 | Parsivel[2] | LPM1 | LPM2 | +1 minute | LPM2/LPM1 |
|---|---|---|---|---|---|---|---|---|---|
| **slope** | 0.9322 | 0.6713 | 0.6397 | 0.9659 | 0.7161 | 0.9409 | 0.9453 | 0.9608 | 0.9194 |
| **std. error** | 7.1705 | 8.8861 | 9.2001 | 9.9617 | 10.0844 | 10.9100 | 10.4077 | 4.7038 | 7.0726 |
| **correlation** | 0.8294 | 0.6275 | 0.5815 | 0.7221 | 0.5995 | 0.6847 | 0.7068 | 0.9231 | 0.8645 |
| **correct type** | 69.5% | 77.5% | 76.4% | 67.8% | 69.2% | 59.1% | 59.7% | 93.8% | 88.5% |
| **correct class** | 97.0% | 97.0% | 95.3% | 95.1% | 97.0% | 96.4% | 96.3% | 98.7% | 97.4% |
| **correct y&n** | 98.1% | 95.9% | 95.6% | 96.0% | 95.8% | 95.2% | 95.7% | 99.0% | 95.8% |

Note that Table 3 also gives the result for the FD12P data, but shifted 1-minute in time, compared to the original FD12P data and the results for LPM2 versus LPM1. When the 1-minute precipitation type, reported by the FD12P but delayed by 1-minute, is compared to the original FD12P data, the agreement as given by the quantities considered in Table 3 is the best. The largest improvements occur for the standard error, the correlation coefficient and "correct type". These numbers give an indication of the effect of the time synchronisation of the sensor data on the scores. The results for LPM2 versus LPM1 give an indication of the reproducibility of the sensor results. Note that both LPMs are mounted on the same mast, but point in opposite directions. This sensor setup has been used in the past to investigate the dependency of the sensor results on the wind speed and direction. The agreement between LPM2 and LPM1 is generally of the same order as the agreement between PWD22 and FD12P, which can also be considered two similar instruments, but "correct type" shows better agreement.

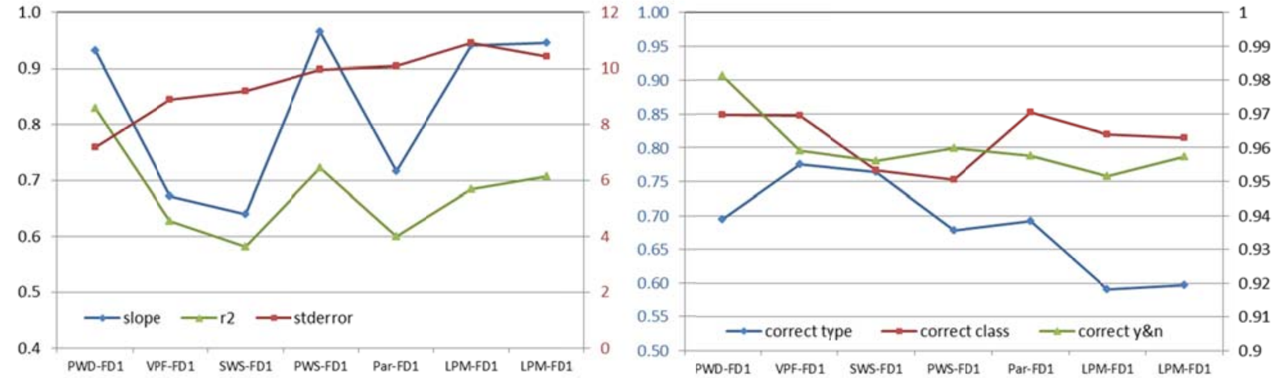


**Figure 3: The slope of the linear regression, the standard error of the linear fit and the correlation coefficient of the 1-minute precipitation type reported by a PWS versus the FD12P (left) and the percentage of cases in correct classes (right).**

**Table 4: POD, FAR and BIAS scores for the classes unidentified, liquid, freezing and solid precipitation and precipitation detection of a PWS compared to the FD12P.**

| Score | PWD22 | VPF750 | SWS250 | PWS100 | Parsivel[2] | LPM1 | LPM2 | +1 minute | LPM2/LPM1 |
|---|---|---|---|---|---|---|---|---|---|
| POD detection | 89.8% | 63.5% | 61.6% | 97.7% | 73.6% | 96.1% | 96.1% | 96.5% | 90.3% |
| FAR | 5.7% | 0.3% | 4.1% | 27.3% | 16.1% | 29.8% | 26.7% | 3.5% | 5.8% |
| BIAS | 0.952 | 0.637 | 0.642 | 1.343 | 0.877 | 1.369 | 1.311 | 1.000 | 0.958 |
| POD unidentified | 0.0% | 0.0% | 0.0% | 6.0% | 0.0% | 0.0% | 0.0% | 62.4% | 1.5% |
| FAR | - | - | - | 98.6% | - | 100.0% | 100.0% | 37.6% | 96.2% |
| BIAS | - | - | - | 4.209 | - | 1.905 | 0.776 | 1.000 | 0.407 |
| POD liquid | 90.2% | 63.7% | 60.5% | 97.0% | 74.0% | 96.4% | 96.3% | 96.2% | 93.7% |
| FAR | 8.0% | 1.9% | 5.4% | 23.6% | 18.2% | 29.2% | 27.9% | 3.8% | 4.5% |
| BIAS | 0.981 | 0.649 | 0.640 | 1.269 | 0.905 | 1.361 | 1.336 | 1.000 | 0.981 |
| POD freezing | 0.0% | 0.0% | 0.0% | 0.0% | 0.0% | 0.0% | 0.0% | 90.0% | - |
| FAR | - | 100.0% | - | - | - | - | - | 10.0% | - |
| BIAS | - | 5.800 | - | - | - | - | - | 1.000 | - |
| POD solid | 70.7% | 57.0% | 61.1% | 44.4% | 59.2% | 59.5% | 60.3% | 95.8% | 87.4% |
| FAR | 32.2% | 35.1% | 62.3% | 3.4% | 35.2% | 39.2% | 40.7% | 4.2% | 15.9% |
| BIAS | 1.042 | 0.879 | 1.618 | 0.459 | 0.913 | 0.979 | 1.017 | 1.000 | 1.039 |

The approach that is generally used for the evaluation of precipitation type is the usage of the Probability of Detection (POD) and the False Alarm Rate (FAR) scores for precipitation classes. For each precipitation class, the percentage of the number of cases in the corresponding column area, that is in the solid coloured area of Figure 2, is the POD. The percentage of the number of cases in the row area that is not in the solid coloured area is the FAR. Furthermore the BIAS, the ratio of the number of cases in the row area to the number of cases in the corresponding column area, is considered. Note that these scores can also be determined for precipitation detection, when all precipitation types are considered one class. Table 4 gives the POD, FAR and BIAS for all precipitation classes obtained for a sensor compared to the FD12P. Figure 4 shows the scores for precipitation detection and for solid precipitation. For precipitation detection the scores for PWD22 shows the best agreement with the

FD12P with a POD of 90 % and a FAR of 6 %. The VPF750 and SWS250 have a low POD (62-64 %) since they report less precipitation events (BIAS about 0.6). The PWS100 and LPM have a high POD (96-97 %) and a high FAR (27-30 %) since they report more precipitation events (BIAS about 1.3). The Parsivel$^2$ has a small BIAS of 0.9 and the POD and FAR have intermediate values of 74 and 16 %, respectively. The KNMI precipitation gauge has a POD of 68 %, FAR of 21 % and BIAS of 0.86. The statistics for unidentified precipitation is poor and UP is not reported by all sensors. For the sensors reporting UP the POD is small, so the UP events occurs at different moments. This is also case for the two LPMs. Delaying the FD12P data by 1-minute leads to a FAR of 38 %, indicating that the duration of UP events is generally short. The scores for liquid precipitation are close to those for precipitation detection, since precipitation mostly occurs as liquid precipitation. The scores for freezing precipitation are poor, but are only based on few events reported by 2 sensors only. The scores for solid precipitation also show the best agreement between PWD22 and FD12P with a POD of 71 % and a FAR of 32 %. The typical POD obtained for the other sensors is about 60 % with a FAR of 35 to 40 %. The SWS250 reports more solid precipitation (BIAS 1.6), resulting in a higher FAR of 62 %, but with little effect on the POD compared to other sensors. The PWS100 reports less solid precipitation (BIAS 0.5), resulting in a low FAR (3 %) and a reduced POD (44 %).

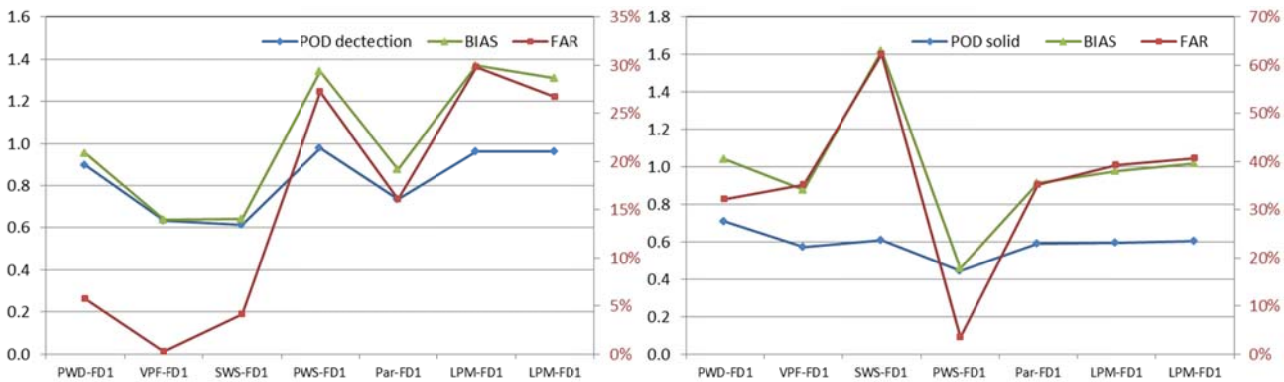


**Figure 4: The POD, FAR and BIAS for precipitation detection (left) and solid precipitation (right) for a PWS compared to the FD12P.**

The above results show that the PWD22 and FD12P generally show the best agreement. This is not surprising since both sensors use the same measurement technique and are from the same manufacturer. Note that the FD12P is not considered the reference. In fact experience showed that the performance of the FD12P could be improved for UP (should not occur or less often), SG (often falsely reported during dense fog), solid precipitation (too few events, particularly during wet snow LRS and hail A). So sensors deviating from the FD12P in these aspects could in fact perform better, assuming that the precipitation that occurred during the evaluation period was representative so that the experiences with the FD12P apply. The contingency matrices of the sensors versus the FD12P show that VPF750, SWS250, Parsivel$^2$ and LPM all report no precipitation when the FD12P reports SG, although some (particularly VPF750 and SWS250) report SG events at other moments. The PWS100 agrees with 5 SG events of the FD12P but reports other events as liquid precipitation (4 cases), UP (20) and clear (104).

Further analysis of the precipitation type results is given for some illustrative cases in section 7. In the remaining of this section, the precipitation type using the WMO 0.02 mm/h threshold is considered. So situations where a PWS reports precipitation type but with intensity ≤ 0.02 mm/h are set to clear. Some results by applying this threshold are given in Table 5. Obviously, this results in a reduced relative occurrence of precipitation for all sensors. The reduction is approximately 1 %, but less for the VPF750 and SWS250 and more for PWS100 and LPM. So the agreement between the sensors improves. Regarding the precipitation classes the FD12P shows the largest change for unidentified precipitation which reduces from 3 to 2 % when the 0.02 mm/h threshold is applied. For the PWS100 the fraction of unidentified precipitation reduces from 10 to 2 %. So the large number of UP events reported by the PWS100 corresponded with low precipitation intensities. When the threshold is applied, the fraction of liquid and solid precipitation events reported by the PWS100 agrees better with the FD12P, although the fraction of solid precipitation is still small. Note that the threshold does not reduce the UP events reported by the LPM much, nor does it affect the high solid precipitation ratio of the SWS250. The scores for precipitation detection agreement increase, except for PWD22 versus FD12P where there is a slight decrease. The highest increases in the agreement with the FD12P is obtained for the PWS100 and Parsivel². The positive BIAS for the PWS100 disappears. For the LPM the FAR decreases significantly. Similar changes are obtained for liquid precipitation. For solid precipitation the POD increases for all sensors, but in particular for the VPF750, SWS250, Parsivel² and LPM. The effect of the threshold on the FAR for solid precipitation is small. The BIAS with respect to the FD12P increases for all PWSs when the threshold is applied, in particular for VPF750 and SWS250.

**Table 5: The relative occurrence of the 1-minute precipitation type reported by the selected present weather sensors and scores for precipitation classes using a 0.02 mm/h threshold.**

| Class / Score | FD12P | PWD22 | VPF750 | SWS250 | PWS100 | Parsivel² | LPM1 | LPM2 |
|---|---|---|---|---|---|---|---|---|
| precipitation | 8.846% | 8.221% | 6.580% | 6.397% | 7.867% | 8.763% | 10.948% | 10.493% |
| unidentified | 2.271% | 0.000% | 0.000% | 0.000% | 1.797% | 0.000% | 4.573% | 1.475% |
| liquid | 95.525% | 97.470% | 96.560% | 94.470% | 96.984% | 97.575% | 93.496% | 96.436% |
| freezing | 0.024% | 0.000% | 0.382% | 0.000% | 0.000% | 0.000% | 0.000% | 0.000% |
| solid | 2.180% | 2.530% | 3.058% | 5.530% | 1.219% | 2.425% | 1.931% | 2.089% |
| POD detection | | 87.1% | 71.4% | 68.9% | 82.1% | 81.2% | 96.6% | 96.5% |
| FAR | | 5.8% | 0.4% | 4.3% | 11.9% | 14.7% | 20.6% | 16.9% |
| BIAS | | 0.925 | 0.717 | 0.720 | 0.932 | 0.952 | 1.217 | 1.161 |
| POD liquid | | 87.0% | 71.0% | 67.2% | 82.3% | 81.0% | 96.5% | 96.2% |
| FAR | | 7.8% | 2.1% | 5.6% | 13.1% | 16.7% | 19.0% | 17.9% |
| BIAS | | 0.944 | 0.725 | 0.712 | 0.948 | 0.973 | 1.191 | 1.172 |
| POD solid | | 73.1% | 64.8% | 69.4% | 49.7% | 67.2% | 67.6% | 68.5% |
| FAR | | 32.3% | 35.1% | 62.0% | 2.7% | 35.2% | 37.2% | 38.6% |
| BIAS | | 1.079 | 0.998 | 1.825 | 0.510 | 1.037 | 1.077 | 1.116 |

## 4. GENERAL OVERVIEW OF THE RESULTS FOR PRECIPITATION INTENSITY

In this section an overview of the results for the 1-minute precipitation intensity reported by the PWSs under evaluation is given. Here the KNMI precipitation gauge serves as the reference. Only situations where either the PWS or the KNMI gauge or both report precipitation are considered. This reduces the number of relevant cases to about 10 to 16 %. Figure 5 gives the relative occurrence of the differences between the 1-minute averaged precipitation intensity of a PWS and the KNMI gauge (PWS−Gauge) using a bin width of 1 mm/h. Table 6 gives some key numbers of these differences and the total precipitation sum obtained by each PWS and the number of precipitation events. The KNMI gauge reported 443.54 mm in 20431 events. FD12P and LPM report much larger precipitation sums, VPF750, SWS250 and PWS100 give much lower sums. The LPM reports many more events with precipitation and the SWS250 much less. Figure 5 shows that the distribution of the differences in precipitation intensity is rather broad. Differences up to ±10 mm/h and more occur. The distribution of the differences in precipitation intensity has a standard deviation of approximately 2 to 3 mm/h. The standard deviation is about 1.5 mm/h for the PWD22 and one LPM. WMO specifies a required measurement uncertainty of ±0.1 mm/h for intensities between 0.2 and 2 mm/h and ±5 % for intensities exceeding 2 mm/h. Traces of precipitation, i.e. intensities between 0.02 and 0.2 mm/h are only relevant for detection of precipitation (yes/no). The percentage of precipitation events where PWS and KNMI gauge agree within the WMO limits of ±0.1 mm/h or ±5 % is typically 38 to 45 % (see Table 6). The LPM has better (60 %) and the SWS poorer (31 %) agreement with the gauge.

Note that KNMI operates the FD12P present weather sensor using the default manufacturer's settings. The manufacturer recommends that the intensity is rescaled with the amount reported by a calibrated rain gauge during a field comparison over a suitable period. This is not easy to handle in practice and therefore not done by KNMI. The precipitation intensity of the FD12P is only used qualitatively by KNMI. This explains the large differences that can occur between the FD12P and KNMI gauge. The same may apply to some other PWS. The precipitation intensity of the Parsivel² and LPM, however, is calibrated by the manufacturer. Rescaling the precipitation intensity of the PWS so that the sums match that of the KNMI gauge does not take account of the variability. The 1-minute precipitation intensity reported by the KNMI gauge can also be wrong. At the onset of light precipitation or during solid precipitation the intensity reported by the gauge is delayed because the precipitation needs to be transferred from the collector to the reservoir first in order to be measured.

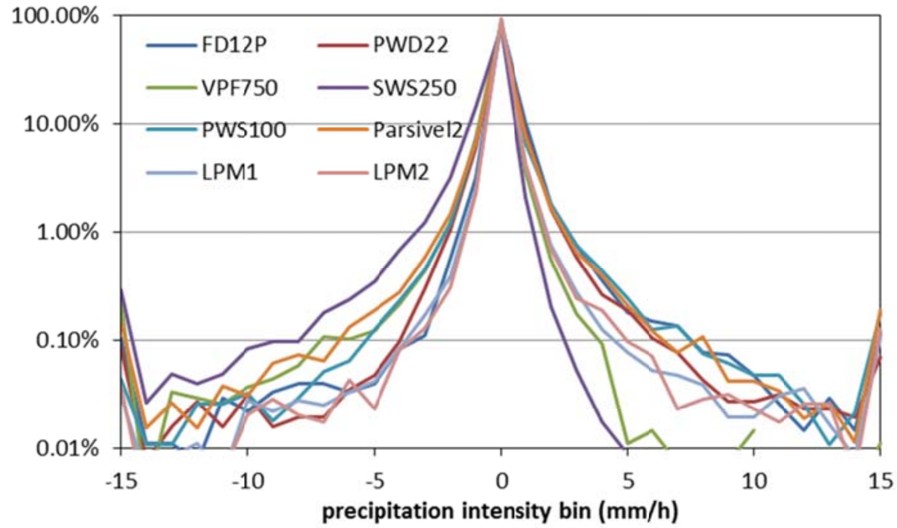


**Figure 5: The relative occurrence of the differences between the 1-minute averaged precipitation intensity of a PWS and the KNMI gauge using a bin width of 1 mm/h.**

**Table 6: Statistics on the differences between the 1-minute averaged precipitation intensity of a PWS and the KNMI gauge (in mm/h).**

| | FD12P | PWD22 | VPF750 | SWS250 | PWS100 | Parsivel$^2$ | LPM1 | LPM2 |
|---|---|---|---|---|---|---|---|---|
| **sum (mm)** | 506.92 | 469.17 | 331.93 | 249.18 | 378.32 | 451.83 | 492.24 | 499.54 |
| **# precipitation** | 22858 | 20676 | 21652 | 15268 | 22695 | 20435 | 32527 | 31256 |
| **# either** | 27495 | 25698 | 27279 | 22879 | 27698 | 26337 | 36209 | 34857 |
| **minimum** | -134.50 | -57.66 | -133.27 | -130.25 | -43.70 | -82.86 | -40.39 | -57.46 |
| **0.05%** | -46.30 | -20.37 | -62.39 | -69.46 | -14.42 | -27.06 | -11.55 | -11.14 |
| **0.5%** | -2.98 | -3.06 | -6.94 | -9.92 | -4.15 | -6.20 | -2.47 | -2.15 |
| **2.5%** | -0.82 | -1.23 | -1.59 | -3.14 | -1.42 | -1.79 | -0.63 | -0.59 |
| **5%** | -0.42 | -0.75 | -0.89 | -1.90 | -0.85 | -0.99 | -0.34 | -0.31 |
| **10%** | -0.19 | -0.39 | -0.49 | -1.04 | -0.45 | -0.48 | -0.17 | -0.17 |
| **25%** | -0.06 | -0.12 | -0.18 | -0.41 | -0.12 | -0.12 | -0.06 | -0.06 |
| **50%** | 0.04 | -0.01 | -0.06 | -0.12 | 0.00 | 0.01 | 0.01 | 0.01 |
| **75%** | 0.25 | 0.18 | 0.05 | -0.06 | 0.10 | 0.17 | 0.10 | 0.10 |
| **90%** | 0.70 | 0.57 | 0.22 | 0.09 | 0.54 | 0.58 | 0.29 | 0.30 |
| **95%** | 1.20 | 1.02 | 0.46 | 0.26 | 1.19 | 1.14 | 0.57 | 0.58 |
| **97.5%** | 2.08 | 1.73 | 0.79 | 0.47 | 2.26 | 2.03 | 1.02 | 1.03 |
| **99.5%** | 6.61 | 5.10 | 2.15 | 1.24 | 7.27 | 7.09 | 4.20 | 4.31 |
| **99.95%** | 18.60 | 17.63 | 8.27 | 3.04 | 40.27 | 27.76 | 25.68 | 28.05 |
| **maximum** | 27.80 | 31.92 | 160.72 | 10.44 | 106.67 | 262.78 | 104.73 | 197.77 |
| **average** | 0.138 | 0.057 | -0.219 | -0.510 | 0.090 | 0.048 | 0.082 | 0.094 |
| **std. dev.** | 2.437 | 1.422 | 2.824 | 2.899 | 2.087 | 2.867 | 1.569 | 1.952 |
| **skew** | -30.688 | -7.417 | -17.270 | -24.598 | 19.521 | 33.051 | 25.074 | 41.705 |
| **WMO** | 42.98% | 39.43% | 44.94% | 30.96% | 44.79% | 37.83% | 59.75% | 59.51% |

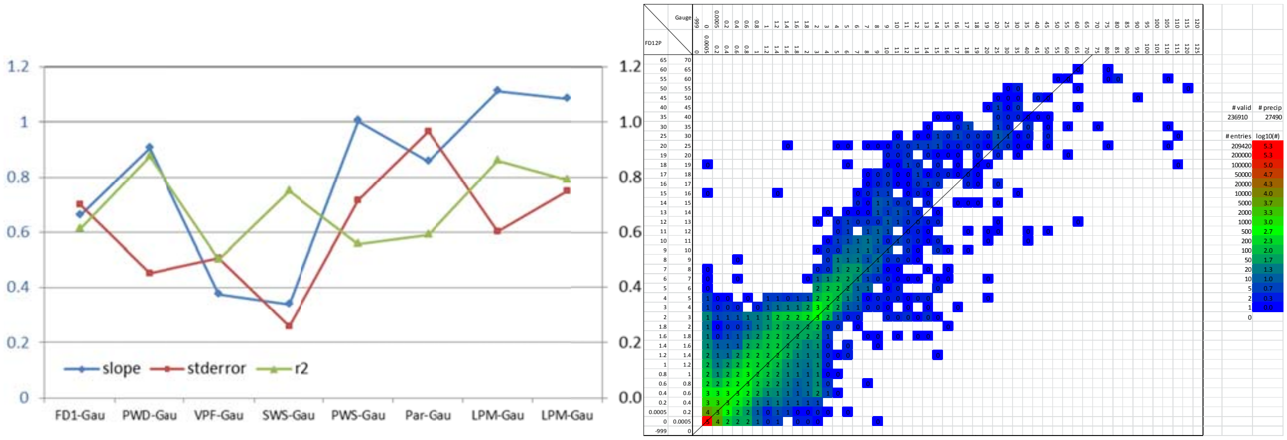


**Figure 6: The slope of the linear regression, the standard error of the linear fit and the correlation coefficient of the 1-minute precipitation intensity reported by a PWS versus the KNMI gauge (left) and a density plot of the 1-minute precipitation intensity reported by the FD12P versus the KNMI gauge (right).**

The 1-minute precipitation intensity reported by the PWSs can also directly be compared to the 1-minute precipitation intensity of the KNMI gauge. Here again only cases when either sensor reports precipitation are considered. The agreement can be expressed in terms of the slope of the linear regression, the standard error of the linear fit and the correlation coefficient. The results are shown in Figure 6. The standard error is lowest for SWS250 and the correlation is reasonably good, but the slope is poor. The slope is best for PWS100 but its correlation is poor. The PWD22 has the best correlation. The Parsivel$^2$ has a poor standard error. Comparing the 1-minute precipitation intensity in this manner seems not so suitable since the variability of the 1-minute precipitation intensity is large. Figure 6 shows a density plot of the precipitation intensity reported by the FD12P and the KNMI gauge. The bin width is 0.2 up to 2 mm/h; 1 up to 20 mm/h and 5 mm/h for higher intensities. A large scatter is evident from Figure 6. Results are also affected by the large number of events at low intensities.

**Table 7: POD, FAR and BIAS scores for precipitation detection (without and with threshold) and for precipitation intensity classes corresponding to light, moderate, heavy and violent rain obtained by from PWS versus KNMI gauge.**

| Score | FD12P | PWD22 | VPF750 | SWS250 | PWS100 | Parsivel$^2$ | LPM1 | LPM2 |
|---|---|---|---|---|---|---|---|---|
| POD 0.0005-9999 | 77.3% | 74.8% | 70.0% | 62.2% | 69.1% | 68.4% | 81.8% | 81.6% |
| FAR | 30.9% | 26.1% | 33.9% | 16.7% | 37.8% | 31.7% | 48.6% | 46.6% |
| BIAS | 1.119 | 1.012 | 1.060 | 0.747 | 1.111 | 1.000 | 1.592 | 1.530 |
| POD 0.03-9999 | 74.9% | 72.0% | 67.0% | 61.6% | 61.4% | 67.6% | 76.1% | 76.0% |
| FAR | 27.0% | 24.5% | 28.5% | 16.5% | 28.7% | 27.6% | 34.9% | 32.4% |
| BIAS | 1.026 | 0.954 | 0.937 | 0.738 | 0.861 | 0.933 | 1.169 | 1.125 |
| POD 0.03-2.5 | 67.5% | 65.4% | 62.1% | 56.5% | 55.4% | 60.6% | 71.3% | 71.2% |
| FAR | 32.4% | 30.3% | 34.5% | 25.7% | 35.1% | 34.4% | 39.9% | 37.3% |
| BIAS | 0.999 | 0.938 | 0.948 | 0.760 | 0.854 | 0.924 | 1.186 | 1.135 |
| POD 2.5-10 | 81.1% | 75.2% | 68.1% | 45.1% | 49.9% | 61.2% | 80.9% | 82.5% |
| FAR | 33.6% | 29.2% | 24.2% | 25.8% | 46.1% | 39.9% | 21.1% | 19.9% |
| BIAS | 1.220 | 1.062 | 0.898 | 0.608 | 0.925 | 1.018 | 1.026 | 1.030 |
| POD 10-50 | 81.9% | 81.6% | 47.6% | 27.6% | 38.4% | 52.1% | 77.5% | 81.0% |
| FAR | 41.4% | 30.0% | 21.1% | 26.3% | 53.8% | 44.4% | 29.3% | 27.8% |
| BIAS | 1.397 | 1.165 | 0.603 | 0.375 | 0.832 | 0.937 | 1.095 | 1.121 |
| POD 50-9999 | 42.3% | 65.4% | 0.0% | 0.0% | 11.5% | 61.5% | 88.5% | 88.5% |
| FAR | 21.4% | 34.6% | 100.0% | - | 83.3% | 38.5% | 32.4% | 28.1% |
| BIAS | 0.538 | 1.000 | 0.038 | - | 0.692 | 1.000 | 1.308 | 1.231 |

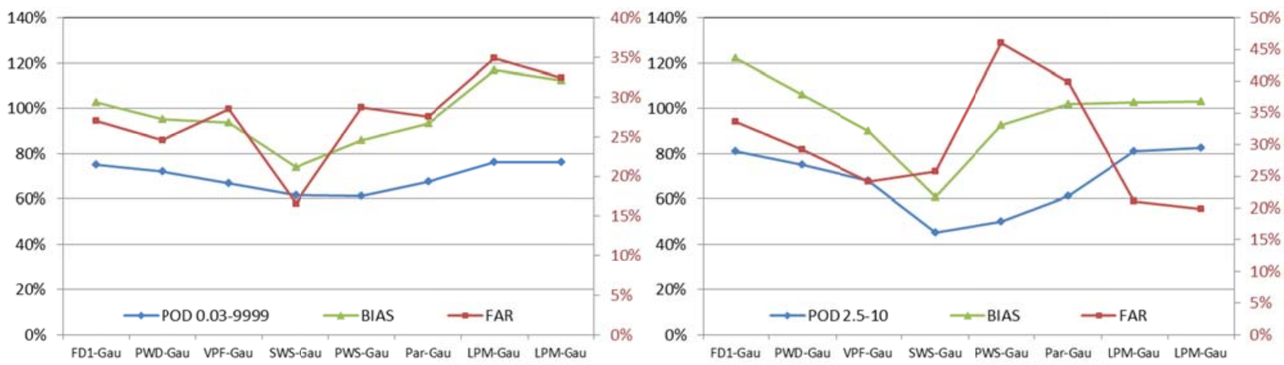


**Figure 7: The POD, FAR and BIAS for precipitation detection using threshold (left) and moderate precipitation (right) for a PWS compared to the KNMI gauge.**

Clearly the differences between the precipitation intensity of a PWS and the KNMI rain gauge cannot always be adequately expressed in terms of averaged values and the standard deviation. The spatial and temporal variability of intensity and the large number of events with low intensity make such an approach unsuitable. The users are often interested in specific intensity classes. The agreement for these classes is then again expressed in terms of POD, FAR and BIAS that are related to the occurrence or not of these specific events. Table 7 gives the scores for the 1-minute precipitation intensity of a PWS versus the KNMI gauge using the reporting limits for light precipitation (intensity below 2.5 mm/h); moderate precipitation (intensity between 2.5 and 10 mm/h); heavy precipitation (intensity between 10 and 50 mm/h) and violent precipitation (intensity equal to or exceeding 50 mm/h). Furthermore, precipitation detection without (intensity exceeding zero) and with threshold (intensity equal to or exceeding 0.03 mm/h) are considered. The scores for detection (see Table 7 and Figure 7) can be compared the those obtained from the precipitation type (cf. Table 4 without and Table 5 with threshold). The individual PWS are now compared to the KNMI gauge, which results in smaller POD values, except for VPF750, with less variability of the POD between the sensors. The BIAS is generally better and also varies less between the sensors. The FAR is always larger when the gauge is used as reference. Compared to the KNMI gauge the SWS250 is the only sensor that shows lower FAR and BIAS values than the other PWS. This could be expected since the SWS250 reports less precipitation events, but the POD is hardly affected. When moderate precipitation is considered the sensors show large variations in the scores compared to the KNMI gauge. The FAR for PWS100 and Parsivel$^2$ increases whereas it decrease for the LPM. The BIAS also changes compared to precipitation detection, suggesting that deviations are a function of precipitation intensity.

## 5. GENERAL OVERVIEW OF THE RESULTS FOR VISIBILITY

In this section, an overview of the results for the 1-minute visibility (Meteorological Optical Range, MOR) reported by the PWSs under evaluation is given. Here the FD12P serves as the “reference” against which the other sensors are compared since it covers a large visibility range. The Vaisala Mitras transmissometer (TMM) can only serve as the reference for visibility values up to 2 km. For MOR it is illustrative to show the occurrence frequency distribution first (cf. Figure 8). The Parsivel$^2$ and LPM show reduced numbers for small MOR. This is not surprising since these sensors report the MOR only during precipitation. Thus in case of no precipitation, no MOR is reported by these sensors (the upper limit of 20000 and 99999 m is in fact reported). In case of precipitation (only in about 10 % of all cases) the visibility reduction that is caused by the precipitation particles is reported. Also note that the frequency distribution of the Parsivel$^2$ and LPM miss the enhanced numbers for MOR below 1 km, because fog is not detected by these disdrometers. The general behaviour is shown by the FD12P, PWD22, VPF750 and SWS250, but the range of the PWD22 is limited to 20 km. The PWS100 shows enhanced numbers for MOR in the range between 500 to about 10 km. The TMM shows values that are gradually increasing compared to the general behaviour between about 2500 m and 15 km, above 20 km the numbers decline rapidly.

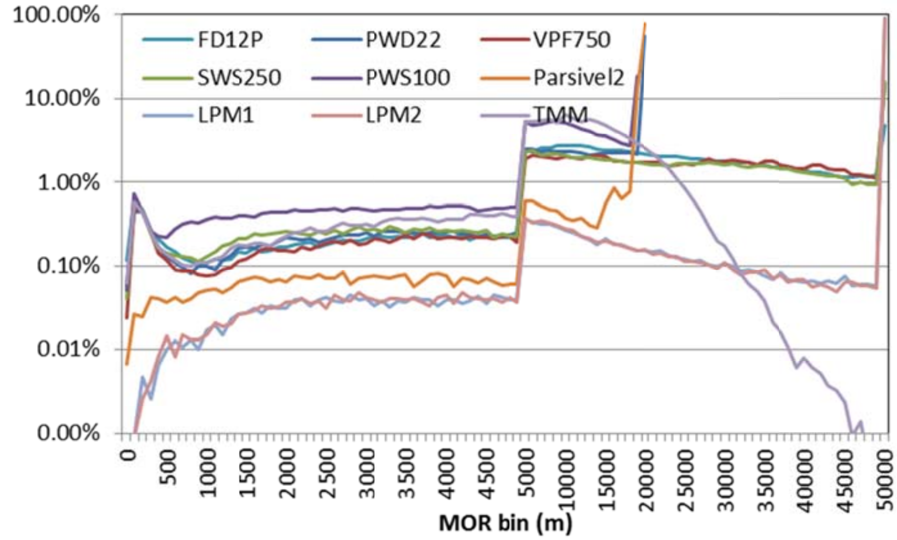


**Figure 8: The frequency distribution of the 1-minute averaged MOR reported by the PWSs and TMM using a using a bin width of 100 m for MOR up to 5 km and 1000 m for higher MOR values.**

Figure 9 gives the relative occurrence of the differences between the 1-minute averaged MOR of a PWS and the FD12P (PWS−FD12P) using a bin width of 1 km. Table 8 gives some key numbers of these differences. Figure 9 shows that the distribution of the differences in MOR is very broad and anti-symmetric. The latter is partly determined by the maximum range of the sensors. So the left side of the PWD22 and PWS100 distribution and the right side for VPF750 and SWS250 have enhanced values. The PWS100 has a strong negative bias. The distribution of the differences in MOR has a standard deviation of about 10 km for PWD22, VPF750, SWS250 and PWS100. WMO specifies a required measurement uncertainty of ±50 m for MOR up to 600 m; ±10 % for MOR between 600 and 1500 m and ±20 % for MOR above 1500 m. The percentage of cases where PWS and FD12P agree within the WMO limits is 43, 49 and 52 %, for PWD22, VPF750 and SWS250, when the visibility of the Birals is limited to 50 km (so MOR above 50 km is set to 50 km). The agreement for the PWD22 is affected by the limited range of 20 km. When the MOR of the sensors is limited to 20 km about 86, 78 and 79 % agree within the WMO limits with the FD12P. The agreement for the PWS100 is poor due to its large underestimation of the MOR. Limiting the MOR to 20 km also gives an agreement of about 60 % for the Parsivel$^2$ and LPM, but only because MOR is often above 20 km and without precipitation, the disdrometers report 20 km.

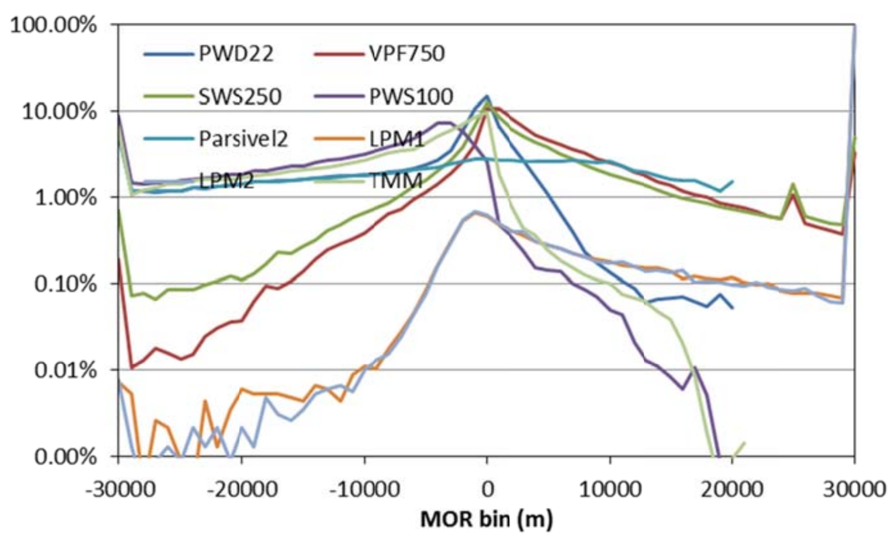


**Figure 9: The relative occurrence of the differences between the 1-minute averaged MOR of a PWS and the FD12P using a bin width of 1 km.**

**Table 8: Statistics on the differences between the 1-minute averaged MOR of a PWS and the FD12P (in m).**

| | PWD22 | VPF750 | SWS250 | PWS100 | Parsivel$^2$ | LPM1 | LPM2 |
|---|---|---|---|---|---|---|---|
| # | 236803 | 226433 | 236802 | 235393 | 222916 | 232574 | 232417 |
| **minimum** | -48784 | -49740 | -49630 | -49862 | -49856 | -39609 | -43071 |
| **0.05%** | -34214 | -46290 | -46870 | -42714 | -46602 | -16385 | -12155 |
| **0.5%** | -30000 | -18100 | -33120 | -38686 | -34477 | -3213 | -3068 |
| **2.5%** | -30000 | -9040 | -14870 | -33244 | -30000 | 503 | 461 |
| **5%** | -29800 | -5570 | -9510 | -30002 | -30000 | 8550 | 8321 |
| **10%** | -25600 | -2280 | -4810 | -28654 | -26100 | 49999 | 49999 |
| **25%** | -14900 | 360 | -590 | -19348 | -15200 | 59599 | 59699 |
| **50%** | -2688 | 3170 | 2000 | -9344 | -2125 | 74799 | 74799 |
| **75%** | 0 | 9390 | 8820 | -3971 | 7300 | 86699 | 86599 |
| **90%** | 1871 | 18740 | 21760 | -1800 | 13770 | 93729 | 93739 |
| **95%** | 3500 | 25400 | 29200 | -686 | 16860 | 96919 | 96929 |
| **97.5%** | 5200 | 31890 | 36140 | 15 | 18640 | 98779 | 98789 |
| **99.5%** | 12540 | 43900 | 47600 | 5857 | 19832 | 99841 | 99841 |
| **99.95%** | 19509 | 54500 | 58100 | 12838 | 19925 | 99921 | 99921 |
| **maximum** | 19869 | 74432 | 73220 | 19736 | 19985 | 99984 | 99984 |
| **average** | -7596 | 5806 | 5012 | -12238 | -4210 | 70015 | 70034 |
| **std. dev.** | 10524 | 9873 | 11986 | 10073 | 14301 | 23229 | 23215 |
| **skew** | -0.801 | 1.111 | 0.831 | -0.681 | -0.320 | -1.446 | -1.449 |
| **WMO 50km** | 43.22% | 48.97% | 51.73% | 4.90% | 19.02% | 15.95% | 15.97% |
| **WMO 20km** | 85.61% | 77.98% | 78.57% | 30.37% | 59.51% | 60.96% | 60.95% |

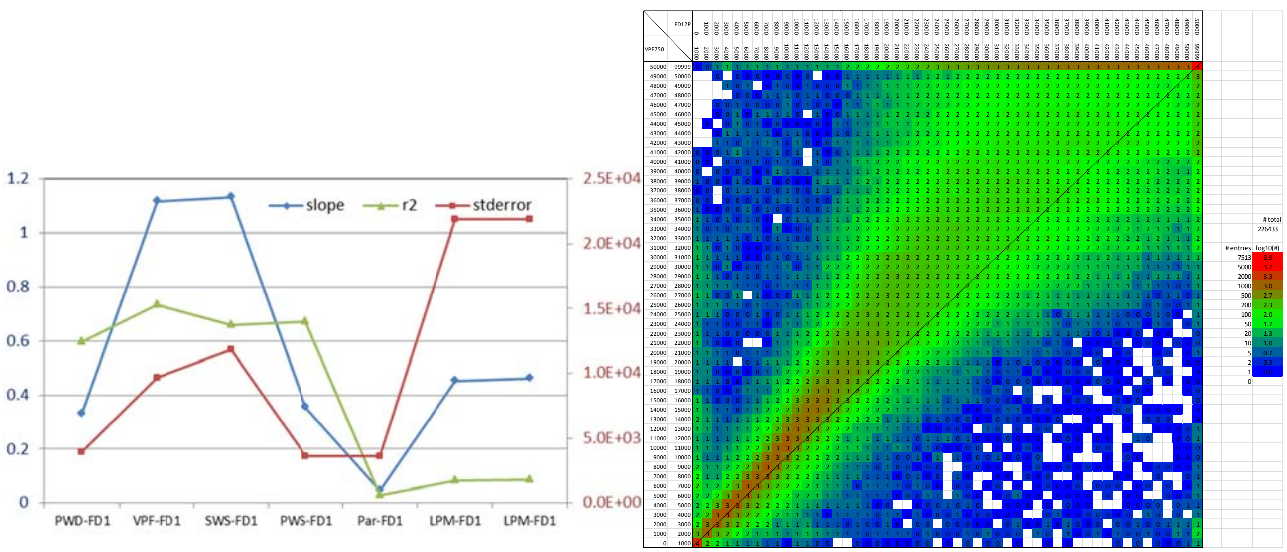


**Figure 10: The slope of the linear regression, the standard error of the linear fit and the correlation coefficient of the 1-minute MOR reported by a PWS versus FD12P (left) and a density plot of the 1-minute MOR reported by the VPF750 versus FD12P (right).**

The 1-minute MOR reported by the PWSs can also directly be compared to the 1-minute MOR of the FD12P. The agreement can be expressed in terms of the slope of the linear regression, the standard error of the linear fit and the correlation coefficient. The results are shown in Figure 10. The MOR values reported by the PWSs have not been limited, so the limited range of a PWS shows up as a slope well below unity and vice versa. The standard error also shows low values for PWD22 and PWS100 and higher values for VPF750 and SWS250. The LPM performs poorly for the standard error. Parsivel[2] and LPM have a low correlation with the FD12P, whereas the other PWSs show little variations. Comparing the 1-minute MOR reported by the PWSs in this manner seems not so suitable since the variability is large. Figure 10 shows a density plot of the MOR reported by the VPF750 and the FD12P. The bin width is 1 km for values up to 50 km. A large scatter is evident from Figure 10. Figure 10 also shows that the VPF750 reports higher MOR values than the FD12P over nearly the entire MOR range.

**Table 9: POD, FAR and BIAS scores for MOR in various visibility classes using the TMM as reference when class limits are below 2 km and the FD12P otherwise.**

| Score | FD12P | PWD22 | VPF750 | SWS250 | PWS100 | Parsivel[2] | LPM1 | LPM2 |
|---|---|---|---|---|---|---|---|---|
| **POD 0-800** | 94.0% | 91.7% | 88.2% | 90.8% | 95.9% | 0.3% | 33.3% | 35.5% |
| **FAR** | 24.4% | 9.8% | 8.6% | 19.4% | 35.6% | 97.8% | 90.1% | 90.8% |
| **BIAS** | 1.244 | 1.017 | 0.965 | 1.127 | 1.490 | 0.130 | 0.028 | 0.030 |
| **POD 800-1500** | 59.0% | 56.6% | 31.6% | 45.6% | 28.1% | 1.2% | 14.6% | 12.2% |
| **FAR** | 41.2% | 39.9% | 58.9% | 65.0% | 90.8% | 97.0% | 86.4% | 89.2% |
| **BIAS** | 1.003 | 0.942 | 0.768 | 1.302 | 3.062 | 0.383 | 0.140 | 0.147 |
| **POD 1500-3000** | | 72.3% | 51.9% | 60.5% | 20.4% | 4.7% | 21.8% | 22.0% |
| **FAR** | | 37.0% | 46.9% | 57.4% | 92.1% | 88.2% | 76.3% | 76.1% |
| **BIAS** | | 1.148 | 0.977 | 1.419 | 2.595 | 0.401 | 0.198 | 0.200 |
| **POD 3000-5000** | | 66.6% | 57.0% | 58.2% | 7.2% | 7.7% | 22.7% | 24.0% |
| **FAR** | | 38.9% | 42.9% | 49.6% | 96.8% | 75.2% | 56.4% | 55.2% |
| **BIAS** | | 1.091 | 0.995 | 1.150 | 2.280 | 0.311 | 0.167 | 0.173 |
| **POD 5000-8000** | | 64.7% | 53.3% | 55.3% | 6.8% | 5.9% | 19.4% | 19.5% |
| **FAR** | | 34.9% | 36.4% | 40.7% | 96.8% | 75.0% | 62.7% | 62.9% |
| **BIAS** | | 0.994 | 0.837 | 0.930 | 2.084 | 0.238 | 0.136 | 0.141 |
| **POD 8000-999999** | | 97.6% | 98.4% | 95.5% | 75.8% | 97.3% | 99.6% | 99.6% |
| **FAR** | | 2.0% | 3.7% | 3.0% | 0.8% | 15.3% | 15.8% | 15.8% |
| **BIAS** | | 0.996 | 1.022 | 0.984 | 0.764 | 1.149 | 1.183 | 1.183 |
| **POD 0-1000** | 93.2% | 90.3% | 87.5% | 88.9% | 96.1% | 1.3% | 50.5% | 51.5% |
| **FAR** | 24.5% | 10.7% | 8.9% | 21.9% | 43.2% | 92.1% | 67.3% | 69.9% |
| **BIAS** | 1.234 | 1.011 | 0.961 | 1.140 | 1.694 | 0.159 | 0.037 | 0.040 |

The differences between the MOR of a PWS and the FD12P cannot always be adequately expressed in terms of averaged values and the standard deviation. The users are often interested in specific visibility classes. The agreement for these classes is then again expressed in terms of POD, FAR and BIAS that are related to the occurrence or not of these specific events. Table 9 gives the scores for the 1-minute MOR of a PWS versus the reference using the limits for issuing a special aeronautical reports for visibility, i.e. a change of the visibility through one of the thresholds 800, 1500, 3000, 5000 or 8000 m. Furthermore the limit of 1000 m for fog in considered. The FD12P is used as reference, except when the limits of a class are below 2 km, when the TMM is used as reference. In that case, the scores for the FD12P are also included in Table 9. The scores for fog, MOR between 1500 m and 3 km, MOR between 5 and 8 km, and MOR exceeding 8 km are also shown in Figure 11. In all cases the visibility in precipitation reported by the disdrometers has the poorest score and a negative (well below unity) BIAS, unless the visibility class includes the MOR value the disdrometer reports in the absence of precipitation. The POD for fog is about 87 to 96 % for the other PWSs. The FAR varies more widely and follows the BIAS. The large positive BIAS of the PWS100 leads to a high FAR. The FD12P, PWD22, VFP750 and SWS250 compare equally well with the TMM for fog, but a PWS with a better POD has a worse FAR. For the mid-range of MOR values the PWD22 compares best with the FD12P, but the scores of the VFP750 and SWS250 are close. The same is true for the high MOR range. Here the PWS100 has a negative BIAS leading to a low FAR, but also a poor POD.

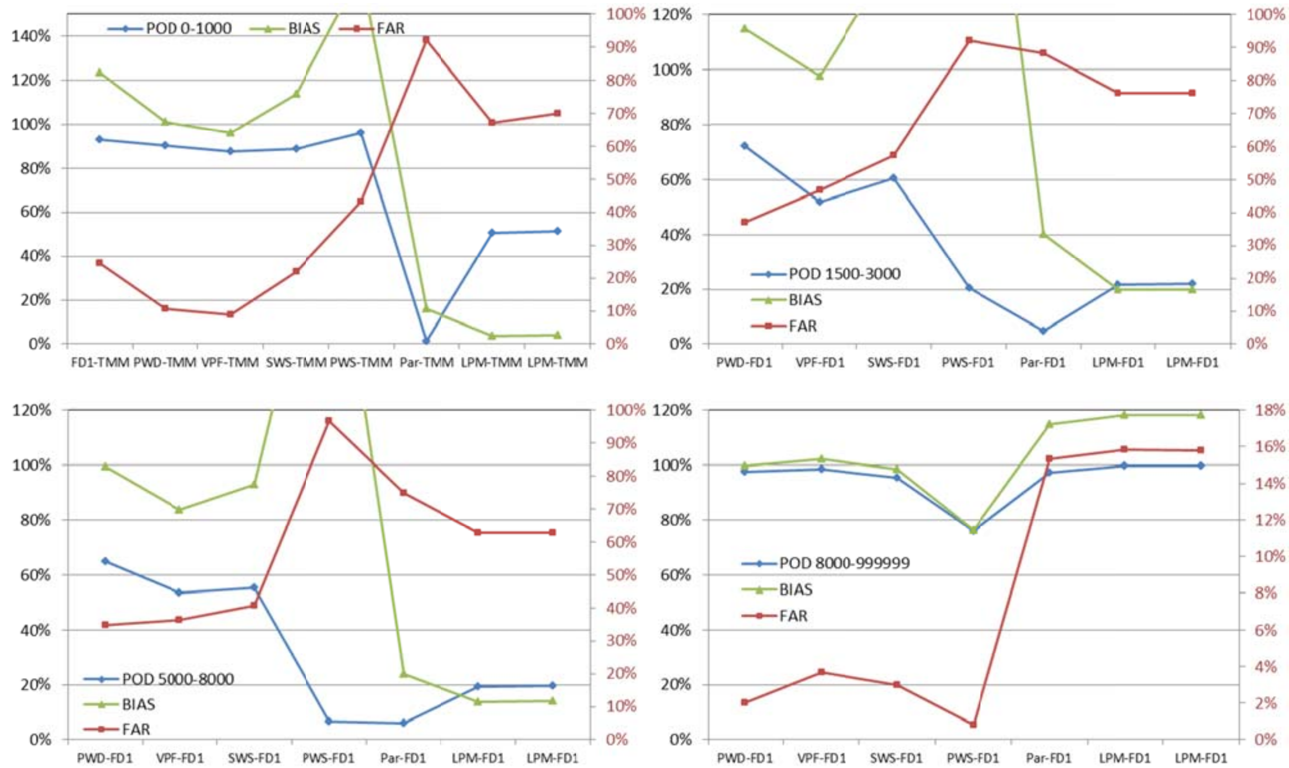

**Figure 11: The POD, FAR and BIAS for fog for a PWS versus TMM (top left) and for low, moderate and high visibility for a PWS versus FD12P.**

In this section all valid 1-minute MOR values have been compared. Note that when the TMM is used as the reference for MOR values up to 2 km, only stable situations (little variability of the MOR) and situations without precipitation are considered. Also the 10-minute averaged MOR (in fact an average of the extinction coefficient, thus average of 1/MOR) is generally used for meteorological applications. Using a 10-minute instead of a 1-minute average will reduce the temporal variability of the MOR values and will reduce the extreme values. The agreement between the MOR reported by the PWSs will generally be better when 10-minute instead of 1-minute averages are considered.

## 6. GENERAL OVERVIEW OF THE RESULTS FOR TEMPERATURE

A PWS is often equipped, or can optionally be extended, with a temperature and sometimes also a humidity sensor. The temperature sensor is either built into the PWS (FD12P, PWD22, SWS250); external to the PWS (LPM), or event separate from the PWS and located in a radiation screen (VPF750 and PWS100). These sensors use the temperature for the discrimination of the precipitation type. It is not always clear whether the temperature aspect of the discrimination can be performed off-line. This is for example possible for freezing or liquid precipitation, which by can corrected to liquid or freezing using the temperature of the AWS. Temperature is generally also used to verify whether a specific type is possible. For example there is no snow at temperatures above 7 °C. When this correction is performed off-line snow is converted into UP, because the PWS gives no suggestion what it otherwise could be. Hence, evaluation of the temperature of the PWS is useful. Note that the Parsivel[2] uses no temperature in the discrimination of the precipitation type. The sensor reports a temperature, but it is a temperature in the sensor housing to control the heating.

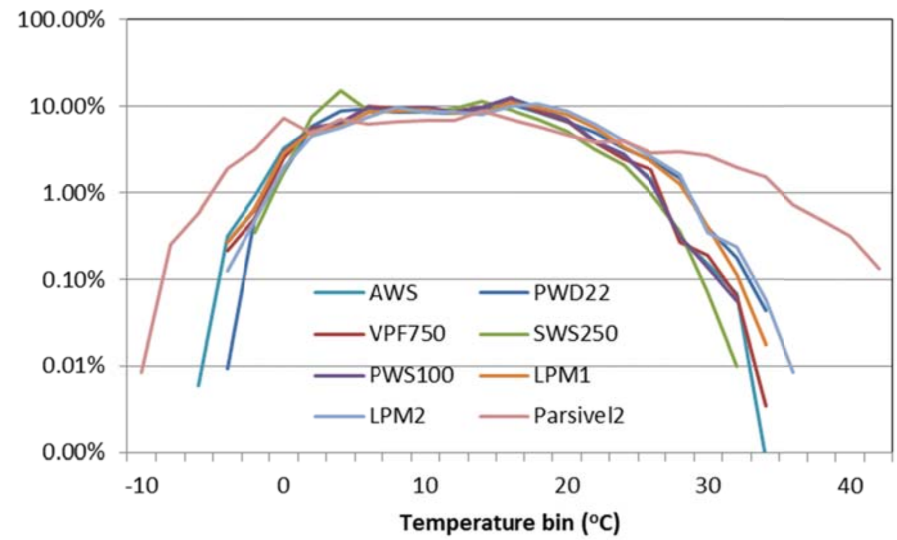


**Figure 12: The frequency distribution of the 1-minute averaged temperature reported by the PWSs and AWS using a using a bin width of 1 °C.**

In this section an overview of the results for the 1-minute temperature reported by the PWSs under evaluation is given. The temperature obtained with the operational temperature sensor of the AWS (at 1.5 m and in a radiation screen) is used as the reference. The frequency distribution of the temperatures obtained by the PWSs and AWS is shown in Figure 12 using a bin width of 1 °C. The Parsivel[2] shows an extended range compared to the other sensors and reports both lower and higher temperatures. Clearly the housing temperature reported by the Parsivel[2] cannot be used as the air temperature.

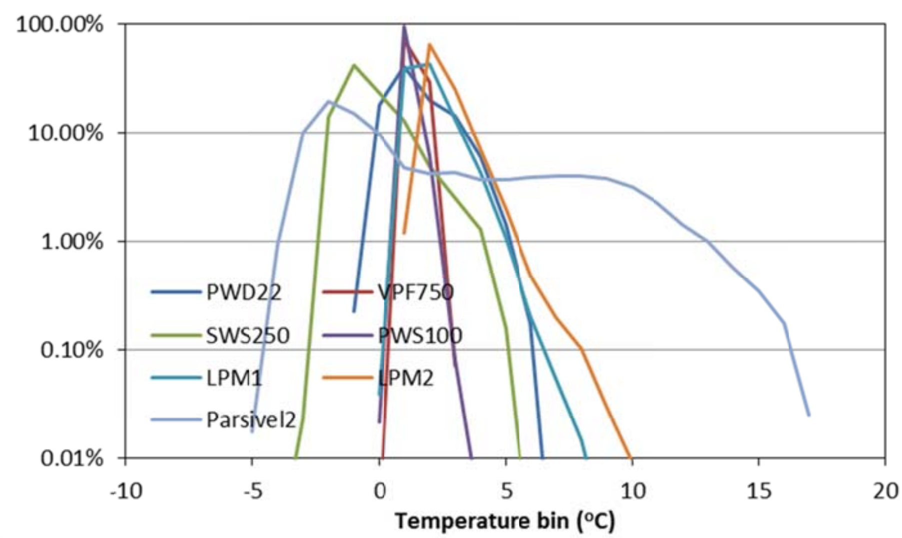


**Figure 13: The relative occurrence of the differences between the 1-minute averaged temperature of a PWS and the AWS using a bin width of 1 °C.**

The relative occurrence of the differences between the 1-minute averaged temperature of a PWS and the AWS (PWS−AWS) is given in Figure 13 using a bin width of 1 °C. Table 10 gives some key numbers of these differences. The distribution of the differences in temperature is very narrow, standard deviation is 0.2 °C, for the VPF750 and PWS100 that use a separate temperature sensor in a radiation screen. The VPF750 and PWS100 have an averaged offset of 0.4 and 0.1 °C, probably because the temperature sensors are at a height of about 2.5 m. The LPMs have a standard deviation of 0.8 °C, but their offset of 0.9 and 1.4 °C is quite large. The temperature sensor of the LPM is external, but located directly underneath the LPM. Hence the temperature may be affect by the LPM. LPM1 is at a height of 1.5 m and the LPM2 at about 20 cm lower, which might explain the offset. The PWD22 and SWS250, with the temperature sensor inside the PWS have the highest standard deviation of 1.2 °C. The PWD22 has an offset of 0.5 °C, the SWS250 has an offset of -1.4 °C. The reason for the large negative offset of the SWS250 is unclear. Both the PWD22 and SWS250 are installed at a height of 2.5 m. Note that the FD12P has a temperature sensor mounted in the mast. This temperature sensor was not available for this test since it is not used operationally. WMO requires a measurement uncertainty of ±1 °C for air temperature. The separate temperature sensors of the VPF750 and PWS100 agree, within the WMO requirements, with the AWS more than 99 % of the time. For the PWD22 and LPM1 agreement is obtained about 70 % of the time. For the SWS250 and LPM2 the agreement is poor as a result of the bias.

**Table 10: Statistics on the differences between the 1-minute averaged temperature of a PWS and the AWS (in °C).**

| | PWD22 | VPF750 | SWS250 | PWS100 | LPM1 | LPM2 | Parsivel[2] |
|---|---|---|---|---|---|---|---|
| # | 236830 | 226459 | 236829 | 235421 | 232602 | 232443 | 222943 |
| **minimum** | -2.5 | -18.1 | -4.9 | -10.5 | -1 | -0.4 | -6.1 |
| **0.05%** | -1.9 | -0.3 | -3.5 | -0.42 | -0.5 | 0.1 | -5.4 |
| **0.5%** | -1.4 | -0.1 | -3.2 | -0.25 | -0.2 | 0.4 | -4.7 |
| **2.5%** | -1.1 | 0 | -3 | -0.17 | 0 | 0.5 | -4.2 |
| **5%** | -0.9 | 0 | -2.8 | -0.13 | 0 | 0.6 | -4 |
| **10%** | -0.8 | 0.1 | -2.7 | -0.09 | 0.1 | 0.7 | -3.6 |
| **25%** | -0.4 | 0.2 | -2.3 | -0.01 | 0.3 | 0.9 | -2.8 |
| **50%** | 0.1 | 0.3 | -1.7 | 0.1 | 0.6 | 1.2 | -1.2 |
| **75%** | 1.3 | 0.5 | -0.7 | 0.22 | 1.2 | 1.7 | 4.3 |
| **90%** | 2.2 | 0.7 | 0.3 | 0.39 | 2 | 2.4 | 8.2 |
| **95%** | 2.7 | 0.8 | 1.1 | 0.54 | 2.5 | 3 | 9.7 |
| **97.5%** | 3.2 | 0.9 | 2 | 0.7 | 3 | 3.5 | 11.1 |
| **99.5%** | 4.1 | 1.2 | 3 | 1.08 | 4 | 5 | 13.6 |
| **99.95%** | 4.8 | 1.5 | 3.7 | 1.64 | 5.8 | 7.3 | 15.2 |
| **maximum** | 5.5 | 2.2 | 4.7 | 2.94 | 7.6 | 9 | 16.5 |
| **average** | 0.483 | 0.352 | -1.381 | 0.131 | 0.861 | 1.402 | 0.849 |
| **std. dev.** | 1.182 | 0.242 | 1.250 | 0.226 | 0.818 | 0.810 | 4.615 |
| **skew** | 0.848 | -1.089 | 1.213 | -0.374 | 1.667 | 2.113 | 0.894 |
| **WMO ±1°C** | 67.63% | 99.04% | 26.53% | 99.30% | 70.61% | 41.68% | 10.88% |

**Table 11: Overview of several quantities indicating the agreement between the 1-minute temperature reported by PWS and AWS, and the POD, FAR and BIAS scores for temperature above and below zero °C.**

| | PWD22 | VPF750 | SWS250 | PWS100 | LPM1 | LPM2 | Parsivel[2] |
|---|---|---|---|---|---|---|---|
| **slope** | 1.0409 | 0.9869 | 0.9455 | 0.9861 | 1.0498 | 1.0525 | 1.4233 |
| **std. error** | 1.1504 | 0.2262 | 1.1972 | 0.2063 | 0.7463 | 0.7312 | 3.6898 |
| **correlation** | 0.9731 | 0.9988 | 0.9650 | 0.9990 | 0.9887 | 0.9892 | 0.8645 |
| **POD 0-98** | 100.0% | 100.0% | 99.9% | 100.0% | 100.0% | 100.0% | 97.6% |
| **FAR** | 0.9% | 0.9% | 1.0% | 0.4% | 0.6% | 1.1% | 0.1% |
| **BIAS** | 1.009 | 1.009 | 1.009 | 1.004 | 1.006 | 1.011 | 0.977 |
| **POD -98+0** | 49.5% | 66.4% | 44.5% | 82.6% | 77.5% | 54.1% | 97.3% |
| **FAR** | 2.9% | 0.0% | 4.5% | 0.0% | 0.4% | 0.0% | 68.6% |
| **BIAS** | 0.510 | 0.664 | 0.466 | 0.826 | 0.778 | 0.541 | 3.099 |

The slope of the linear regression, the standard error of the linear fit and the correlation coefficient of the 1-minute temperature reported by a PWS versus AWS is shown in Figure 14 and reported in Table 11. The results are again as could be expected from the location of the temperature sensor. The VPF750 and PWS100 have the lowest standard error and a correlation coefficient closest to unity. The LPM is again third best followed by PWD22 and SWS250. The standard deviation seems the best indicator of the quality of the temperature measurements of the PWS. The slope is not always a good indicator of the averaged offset, since a steeper slope does not always correspond to a more positive offset or vice versa.

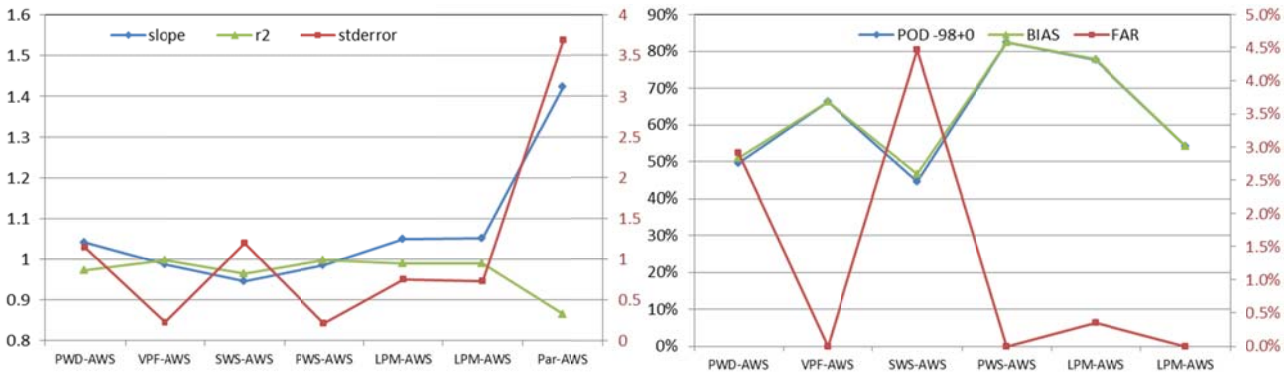


**Figure 14: The slope of the linear regression, the standard error of the linear fit and the correlation coefficient of the 1-minute temperature reported by a PWS versus AWS (left) and POD, FAR and BIAS scores for temperature below zero °C (right).**

Finally the POD, FAR and BIAS scores for specific classes are considered. The classes temperatures above and temperatures below zero are chosen since they are relevant for the discrimination of non-freezing or freezing precipitation. The results for the scores are given in Table 11. The scores for temperatures above zero are affected by the fact that the temperatures generally are above zero. Hence the POD is high, the FAR is low and the BIAS is close to unity because generally sensors agree that the temperature is above zero. The FAR is typically 1 % and the BIAS is larger than 1 for all sensors, even for the SWS250 that had an averaged offset of -1.4 °C. Also the PWS100 has a lower FAR than the other sensors including the VPF750, although the PWS100 and VPF750 had the same overall agreement with the temperature reported by the AWS. Clearly the differences between PWS and AWS temperature are a function of temperature. The scores for temperatures below zero (see Figure 14) involve less cases and the scores show more variations between the sensors. The results for PWD22, VPF750, SWS250 and PWS100 follow the behaviour of the overall differences with VPF750 and PWS100 having better POD and FAR than PWD22 and SWS250. The POD of PWS100 is better than that of VPF750 (83 versus 66 %), and the FAR of PWD22 is better that of SWS250 ( 3 versus 5 %). The LPM performs relatively better than the overall differences indicated. All sensors have a negative BIAS (values below unity).

## 7. ILLUSTRATIVE CASES

This section gives examples of the measurements of the PWSs for some selected days. The selected days cover various illustrative precipitation events. Figure 15 shows the precipitation type and the accumulation of precipitation intensity on June 23, 2016. The precipitation type is indicated by small vertical bars using the scale on the left. The value of each sensor has a small offset in order to make the results for all sensor visible. The KNMI gauge is also included in Figure 15, but for precipitation type only clear ("C") and precipitation ("UP") is indicated. For precipitation intensity the gauge serves as the reference and is indicated by the thick line. The measurements between 0 and 12 UT are given Figure 15, during which 2 events with summer hail occurred. Between 1 and 2 UT hail ("A") is reported by the VPF750, SWS250, LPM and Parsivel2. VPF750 and SWS250 also report snow pellets ("SP") and the LPM also reports ice pellets ("IP"). The FD12P, PWD22 and PWS100 report rain ("R") in this period. Rain is reported also by the other PWS. Note that the PWS100 data was unavailable during the second half of the event. Shortly after the start of the event the gauge reports 25 mm and at the end of the event the sum is 36 mm. The fast response of the gauge indicates that a large fraction of the precipitation occurred as rain. In fact the gauge showed no indication of delayed precipitation recording due the melting of solid precipitation in the collector. The VPF750 and SWS250 report 11 and 10 mm, the FD12P and PWD22 report 21 and 28 mm, respectively. The calibrated disdrometers give better results with Parsivel$^2$ reporting 34 and LPMs 41 and 40 mm. The PWS results for the second summer hail event around 10 UT gives similar results. The period when sensors report solid precipitation is now much shorter. Note that the PWD22 agrees with the gauge on the precipitation amount of the second event (11 mm).

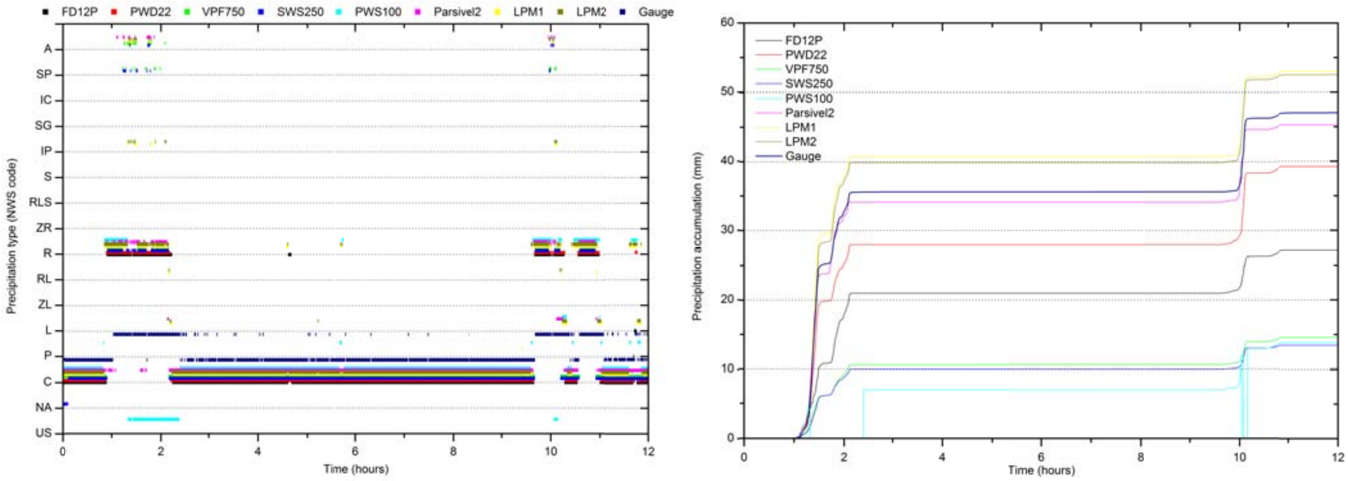


**Figure 15: Plot of the precipitation type (left) and precipitation intensity accumulation (right) for all PWSs and the KNMI gauge on June 23, 2016 between 0 and 12 UT.**

Figure 16 shows the precipitation type and the accumulation of precipitation intensity on June 26, 2016. A summer hail event occurred between 11 and 12 UT. Again hail is reported by the VPF750, SWS250, LPM and Parsivel$^2$, but LPM2 is now the only sensor that also reports another solid precipitation type (ice pellets). A possible second event near 12:30 UT is only reported as such by VPF750 and Parsivel$^2$. The Parsivel$^2$ shows again the best agreement with the gauge, but reports more accumulated precipitation for the first events and less at the second. Compared to Figure 15 LPM2 now reports more than LPM1 and FD12P and PWD22 are closer to each other.

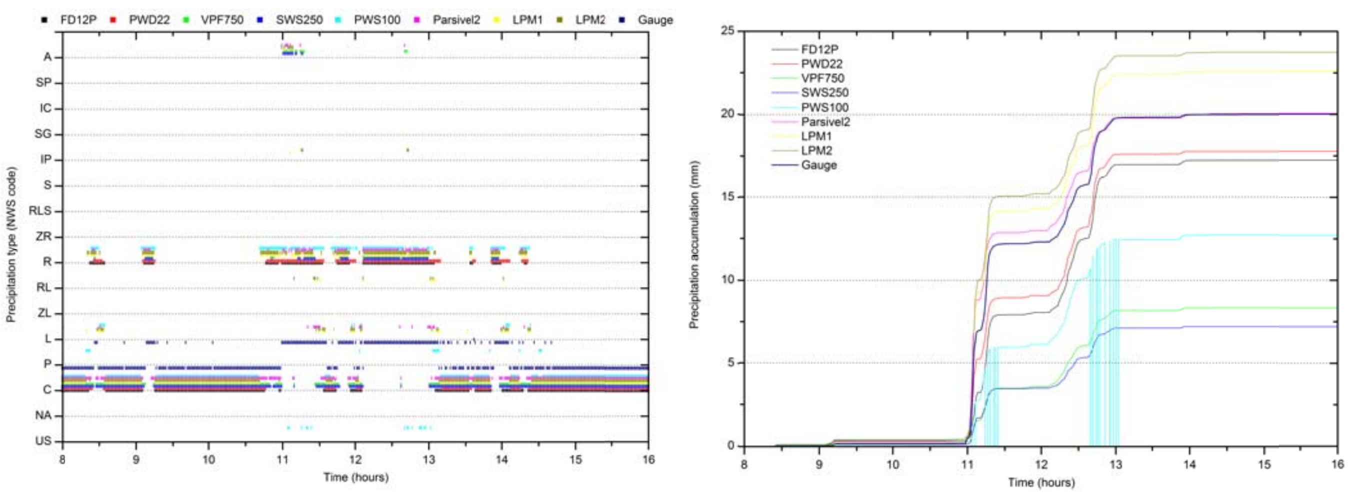


**Figure 16: Plot of the precipitation type (left) and precipitation intensity accumulation (right) for all PWSs and the KNMI gauge on June 26, 2016 between 8 and 16 UT.**

Figure 17 shows the precipitation type and the accumulation of precipitation intensity on February 25, 2016. On this day solid precipitation (snow) occurred. The main events occur at 1:00, 2:30 and particularly at 12:30 UT. At 1 UT all PWS reports snow ("S"). The VPF750 mainly reports a mixture of rain and snow ("RL"). The PWS22 also reports ice pellets and the Parsivel$^2$ also reports snow pellets. The PWS100 reports UP several times during this event. The same behaviour can be observed at 2:30

UT, but now the VPF750 also reports some snow grains ("SG"). At 12:30 UT there is some disagreement between the sensors. VPF750 and SWS250 report mixture of rain and snow, FD12P reports mainly rain but also some snow, PWD22 and LPM report ice pellets and some snow, Parsivel[2] reports snow pellets. All PWSs also report some rain near 12:30 UT, but the PWS100 reports rain (and unidentified precipitation) only. Note that during these precipitation events the temperature reported by all sensors was above zero. During the 12:30 UT event all sensors show a sudden drop of about 3 °C within one minute. On this day the presence of (some) solid precipitation at the three events is also evident from the measurements of the gauge, which showed delayed precipitation as a result of the melting of snow. For example Figure 17 shows all PWS stop reporting precipitation at 12:30 UT, whereas the precipitation sum of the gauge keeps increasing up to 13:10 UT. The high precipitation accumulation reported by the PWS100 is contrary to the results given above.

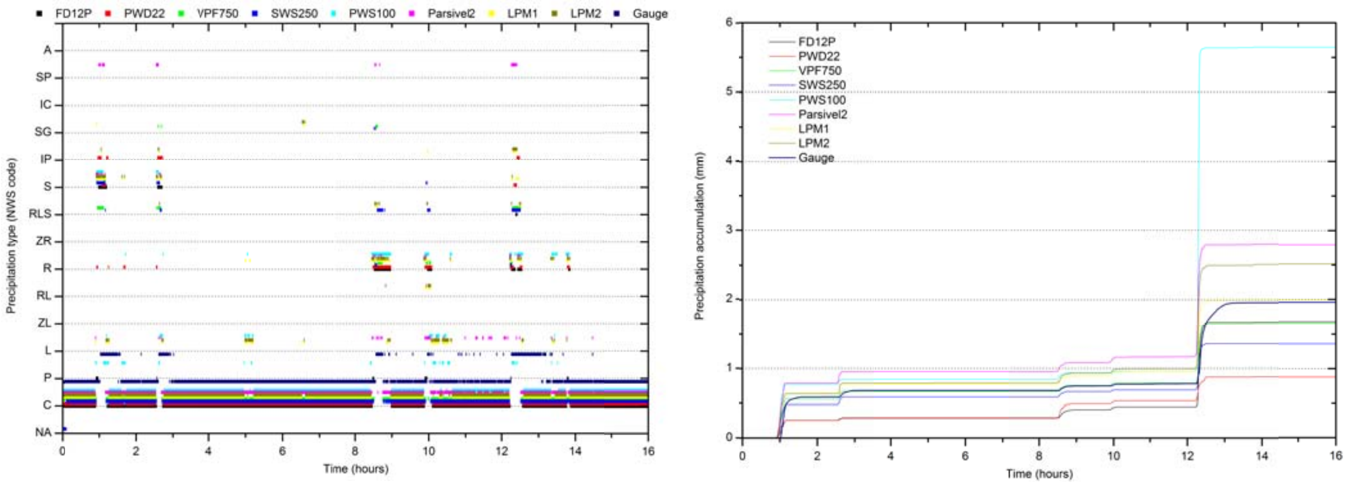


**Figure 17: Plot of the precipitation type (left) and precipitation intensity accumulation (right) for all PWSs and the KNMI gauge on February 25, 2016 between 0 and 16 UT.**

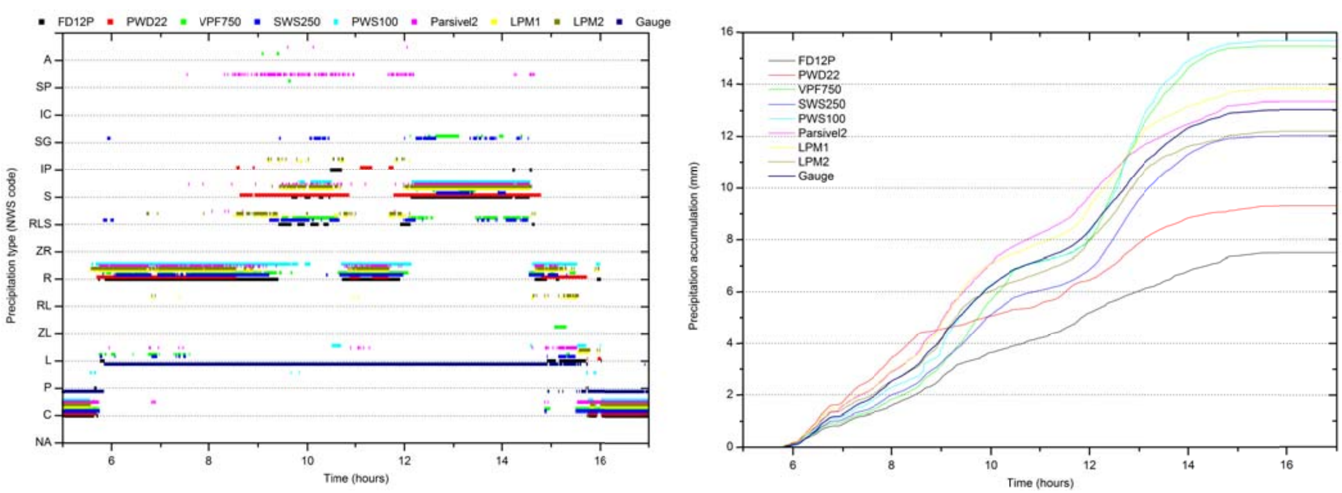


**Figure 18: Plot of the precipitation type (left) and precipitation intensity accumulation (right) for all PWSs and the KNMI gauge on March 4, 2016 between 5 and 17 UT.**

On March 4, 2016 and extensive snow event occurred between 9 to 11 UT and 12 to 15 UT (cf. Figure 18). The first event shows the largest differences in precipitation type reported by the sensors. The PWS22 and LPM are the first sensors that report snow or a mixture of rain and snow. The SWS250, FD12P and VPF750 come next and the PWS200 is last. The Parsivel[2] reported also start reporting solid precipitation early, but it reports mainly snow pellets. The PWS100 switches to snow grains at the end of the event and the FD12P switches to ice pellets. Between 11 and 12 UT the sensors report rain, except for the PWD22 reports ice pellets for some time. The agreement between the PWS is better for the event between 12 and 15 UT. Snow is generally reported. The Parsivel[2] reports snow pellets at the start and end of the event. The VPF750 and SWS250 partly report snow grains during the event. During the entire period all temperatures where between 0.2 and 4 °C, only the SWS250 reports temperatures below zero. This occurs between 12:30 and 13:00 UT and corresponds roughly with the period when the SWS250 reports snow grains. Figure 18 shows that the gauge shows no indication of delayed precipitation. The snow events where followed by rain, which would have melted the snow in the collector.

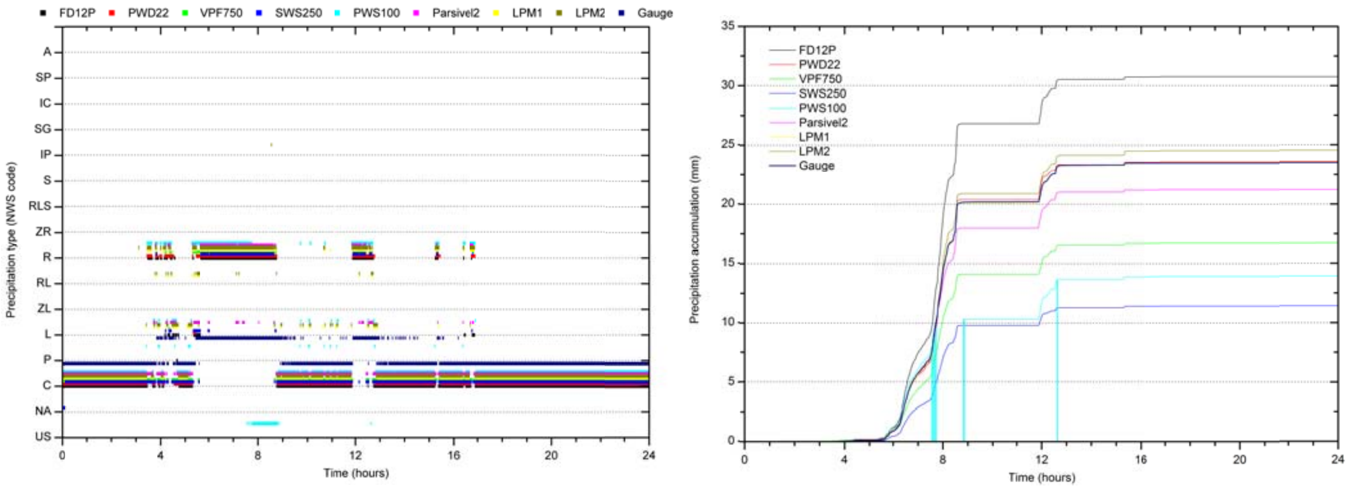


**Figure 19: Plot of the precipitation type (left) and precipitation intensity accumulation (right) for all PWSs and the KNMI gauge on June 14, 2016.**

Figure 19 shows an example of the PWS measurements during rain that occurred on June 14, 2016. Sometimes drizzle is reported by some sensors, but rain clearly dominates for all PWSs. The FD12P now shows an overestimation of the precipitation amount compared to the gauge. The PWD22 and LPMs give good agreement with the gauge and the Parsivel$^2$ has a small underestimation. The VPF750 and SWS250 have again a large underestimation. One hour of data for the PWS100 is missing, otherwise is would have reported an amount close to that of the gauge.

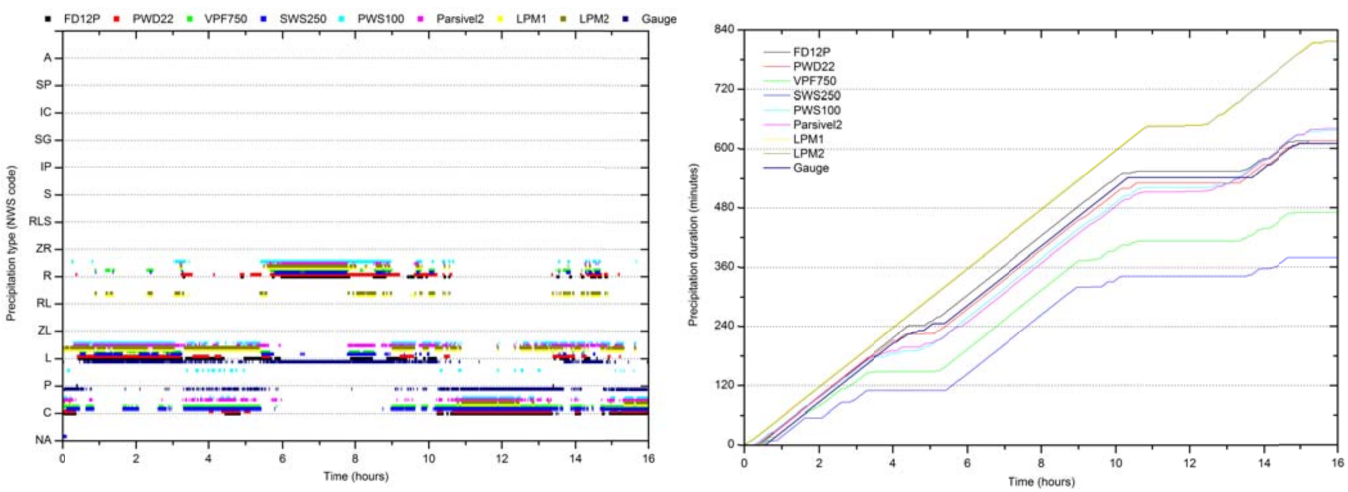


**Figure 20: Plot of the precipitation type (left) and precipitation duration accumulation (right) for all PWSs and the KNMI gauge on March 25, 2016 between 0 and 16 UT.**

The PWS measurements of March 25, 2016 with drizzle are given in Figure 20. Generally there is good agreement between the PWS for reporting drizzle between 0 and 6 UT. Note that the PWS100 reports some unidentified precipitation. The LPMs show some periods with a mixture of drizzle and rain. During these situations the PWD22 and PWS100 mainly report rain and the FD12P and Parsivel$^2$ report drizzle while VPF750 varies. The precipitation duration (here any intensity > 0) is determined by the sensor response between 4 and 5 UT and 10 and 14 UT. The LPMs are the only sensors that report precipitation in the first period, the VPF750 and SWS250 show the largest interval without precipitation. The overall result is that the LPM is more sensitive than the gauge, the VPF750 and SWS250 are less sensitive than the gauge, and the other PWSs have similar sensitivity as the gauge. Note that at the onset of drizzle at the beginning of the day the gauge reacts slowest. Probably this reflects the fact that it takes some time before the drizzle in the collector runs down into the reservoir where it is measured. During the day, when the collector is still wet, this delay it less obvious since some PWS also show longer gaps for detection. At 14 UT the delay of the gauge is visible again.

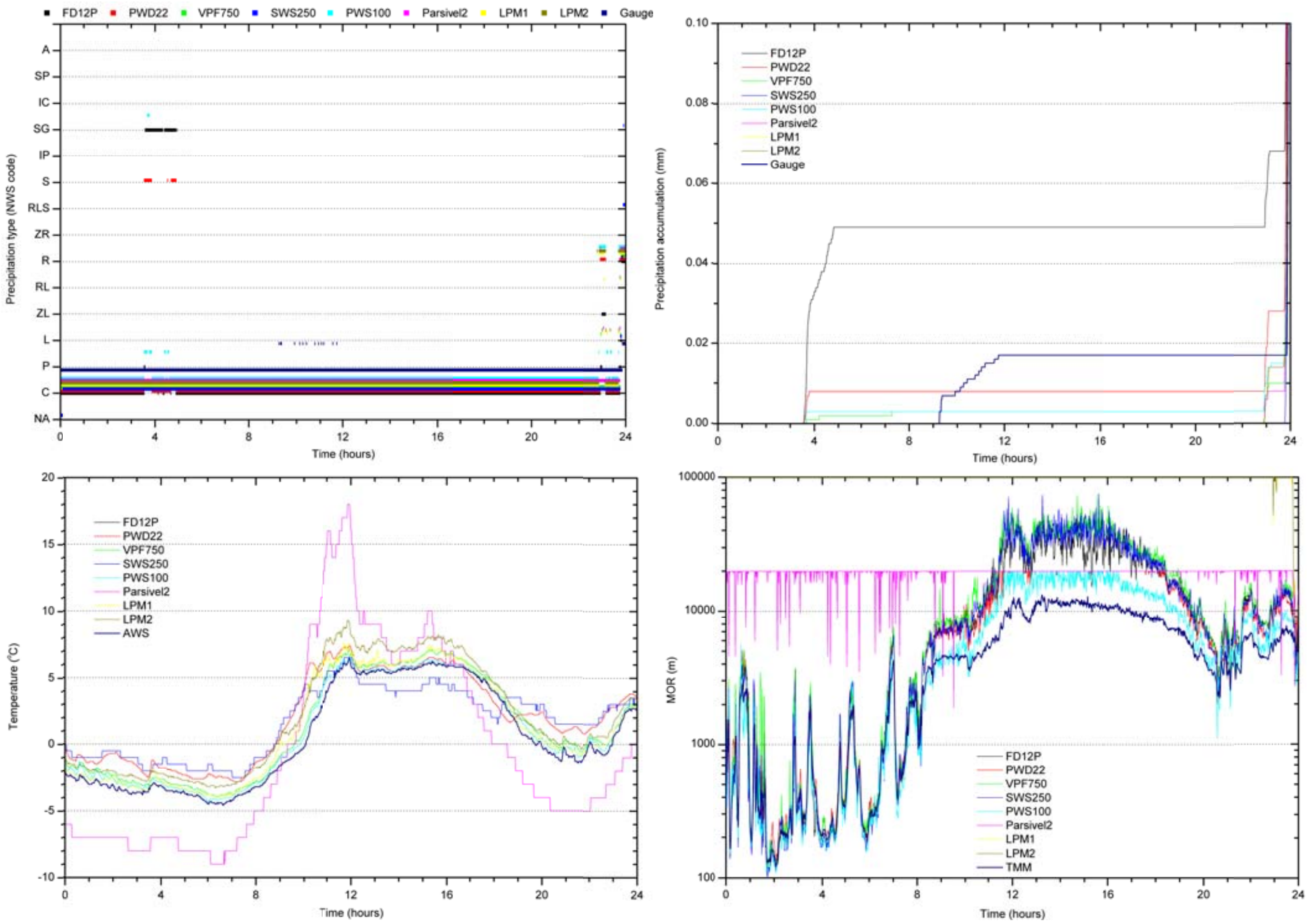


**Figure 21: Plot of the precipitation type (top left), precipitation intensity accumulation (top right), temperature (bottom left) and MOR (bottom right) for all PWSs on March 5, 2016. The measurement of the KNMI gauge, AWS temperature and TMM are indicated by the thick lines.**

The measurements of the PWSs on March 5, 2016 are given in Figure 21. The FD12P reports snow grains between 3:30 and 5 UT during dense fog (MOR below about 300 m). This is a situation where precipitation is probably falsely reported by the FD12P due to fog. The precipitation intensity is low, but above the threshold of 0.02 mm/h. Note that the PWD22 reports snow at the onset and cessation of the snow grains event of the FD12P, whereas the PWS100 reports unidentified precipitation and some snow grains. The associated intensity is very low, but some events exceed the threshold. The other PWSs report no precipitation during the fog event. At 23 UT the FD12P reports freezing drizzle (“ZL”). The other PWSs report drizzle and/or rain, except the SWS250, which reports no precipitation, and the VPF750, that only reports unidentified precipitation just before the FD12P freezing drizzle event. Only six freezing drizzle events reported by the FD12P meet the threshold of 0.02 mm/h. These constitute all freezing precipitation cases reported by the FD12P during the entire period of the field evaluation. So, the number of freezing precipitation cases is not only very small, but they occur in only one event. The temperature of the AWS changed from below to above zero just 2 minutes before the FD12P started reporting freezing drizzle. In the operational situation the type would have been corrected from freezing drizzle into drizzle. Note that between 20 and 23 UT the temperature of the AWS is mostly below zero whereas the temperatures of the other PWSs is higher and often above zero. If liquid precipitation had occurred in this period the PWSs discrimination of freezing or non-freezing precipitation would have differed.

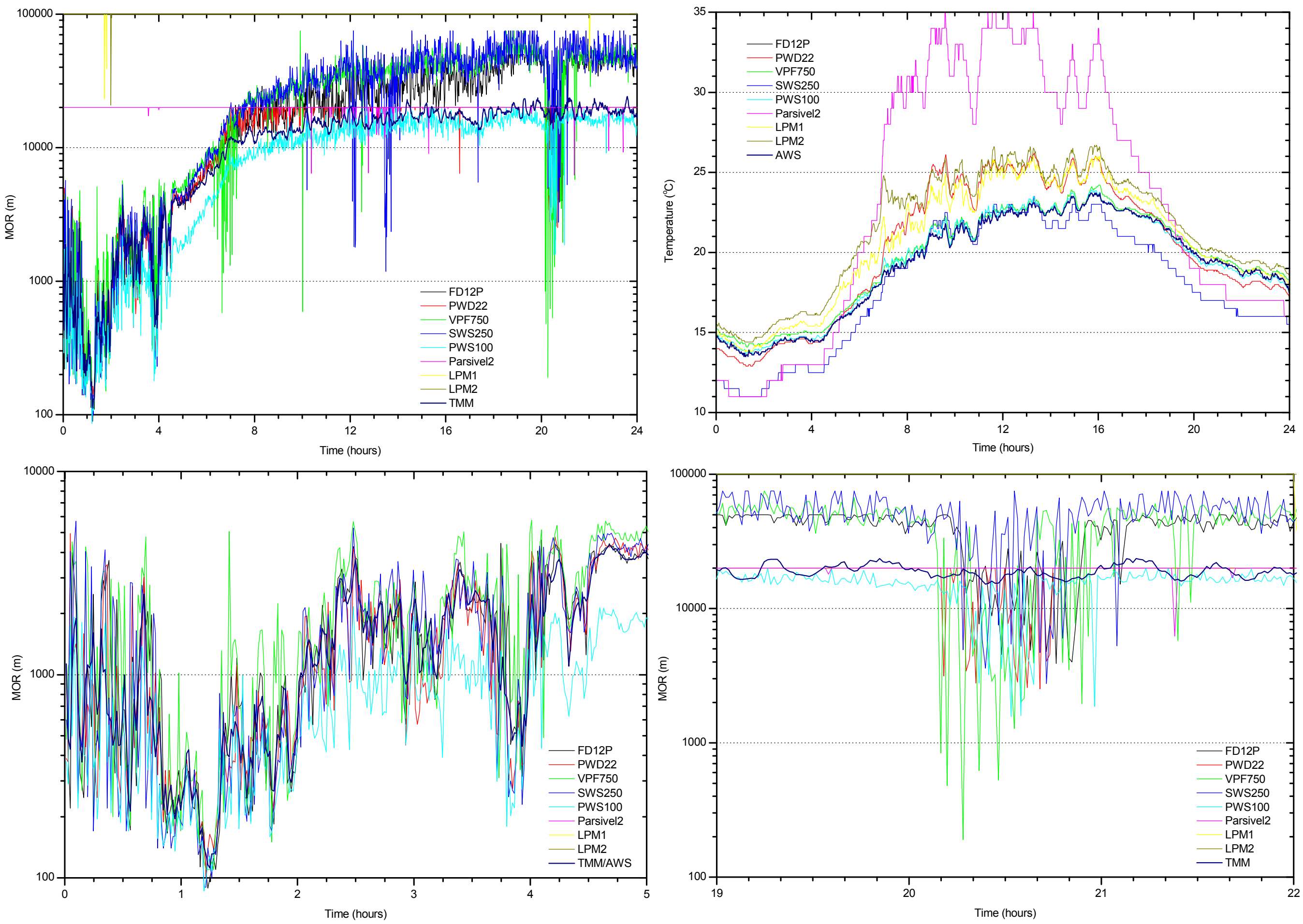


**Figure 22: Plot of the MOR for all PWSs and the TMM on July 9, 2016 showing the entire day (left) and the situation between 0 and 5 UT (lower left) and between 19 and 22 UT (lower right).**

The final case with measurements of the PWSs is not related to precipitation type, but concerns the MOR only. Figure 22 shows the results for July 9, 2016 when fog occurred in the morning. Note that the visibility in precipitation that is reported by Parsivel$^2$ and LPM is included in the graph. These disdrometers do not detect fog and report there default maximum value. Only when the sensor detects precipitation is a visibility reduction, caused by these particles only, reported. The results of the TMM, the reference for visibilities below 2 km, is given by the thick line. When the fog lifts the MOR the TMM increases to about 15 km at about 8 UT and remains there for the rest of the day. The MOR of the forward scatter PWS reaches values of 20 to 50 km during the second half of the day. The MOR range of the PWD22 is 20 km and the sensor reaches this value at noon. The range of the PWS100 is also 20 km, but this values is not reached. Between 5 and 12 UT the PWS100 shows an underestimation of the MOR compared to the other forward scatter PWS. The VPF750 and SWS250 shows some events with reduced MOR values between 5 and 14 UT. During the fog event all visibility sensors report low MOR values. The agreements is good although the VPF750 reports sometimes higher values and the PWS100 reports lower MOR values when MOR is above 1 km. The MOR of all sensors (including TMM) have large fluctuations, so the fog conditions seem to vary. The reduced MOR values between 20 and 21 UT are caused by flying insects. The signal scattered by the insects leads to reduced MOR values. The MOR reported by the TMM is not affected. The insect problem occurs during twilight in calm conditions. Note that MOR reduction varies rapidly from one minute to the next, causing spikes. Some of these spikes (for the VPF750) reach MOR values below 1 km, while the MOR is probably about 50 km. The reason why the MOR of the TMM is not affected by the insects is probably the larger size of the measurement area.

## 8. SUMMARY AND CONCLUSIONS

The evaluation of the precipitation type reported by the PWSs is complicated by the fact that no reference exists. The measurements of the PWSs are compared against the precipitation type reported by the FD12P. The precipitation type reported by FD12P is not always correct, but the characteristics of the FD12P are well known by KNMI after more than 15 years of operational experience and several field evaluations against other sensors and against observers. The preliminary results of the field evaluation regarding precipitation type are:

- The FD12P is generally considered good for precipitation detection. Compared to the FD12P, the VPF750 and SWS250 are less sensitive, the PWS100 and LPM are more sensitive, and the other PWSs have similar sensitivity. Similar results for the sensitivity of the PWSs compared to the FD12P are obtained when a threshold of 0.02 mm/h is applied. The exception is that the PWS100 has a similar sensitivity as the FD12P when the threshold is used.
- The FD12P reports 2 to 3 % of the precipitation as unidentified precipitation, which causes problems for the users. Of the other PWSs only the PWS100 and LPM report unidentified precipitation. The fraction of unidentified precipitation reported by the PWS100 is very high when no intensity threshold is used.
- The FP12P generally reports too few cases of solid precipitation. During the field evaluation period, the PWS100 reports even fewer cases than the FD12P and the SWS250 reports many more solid precipitation cases. The other PWSs report numbers comparable to the FD12P. The PWD22, VPF750 and Pasivel$^2$ report higher and the LPM reports lower numbers than the FD12P.
- The FD12P generally reports too many cases of ice pellets. The FD12P reports only a small number of ice pellets during the field evaluation period. The LPM reports slightly higher numbers. The PWD22 reports much higher numbers, but it does not report any other solid precipitation types except snow and ice pellets. The other PWSs report no ice pellets events.
- Snow grains are often reported by the FD12P during dense fog. When the FD12P reports snow grains during the field evaluation period the other PWSs generally report no precipitation. Only the VPF750 and SWS250 report snow grains, but generally not at moments when the FD12P reports it.
- The FD12P reports hardly any hail or snow pellets. The PWS100 and PWD22 reports no hail or snow pellets. The LPM and SWS250 report higher numbers than the FD12P. The VPF750 reports many more cases than the FD12P and the Parsivel$^2$ reports a very high number of snow pellets.

Overall the PWD22 generally compares best with the FD12P when the scores for the liquid precipitation class are considered. The LPM has a better POD as a result of the higher sensitivity, but also a higher FAR. The PWS100 and Parsivel2 have poorer POD and FAR compared to the PWD22, but the FAR is better than for the LPM. The VPF750 and SWS250 have the poorest POD and best FAR as a result of their low sensitivity. The scores for the solid precipitation class compared to the FD12P are best for PWD22. The VPF750, Parsivel$^2$ and LPM have a slightly worse POD and FAR compared to the score of the PWD22. The PWS100 has a poor POD and the SWS250 has a poor FAR. The best overall agreement between the PWD22 and FD12P could be expected as the sensors use the same measurement technique and are from the same manufacturer. However, the FD12P is not necessarily correct. The PWD22 scores deviate more from the FD12P for specific precipitation types, especially since the PWD22 reports the fewest number of precipitation types. Also note that the although the scores for the liquid precipitation class is generally good, the discrimination between rain and drizzle varies largely between the PWSs.

The precipitation intensity reported by the PWSs is compared to the intensity obtained with a KNMI gauge. All PWSs report precipitation intensity, but only the Parsivel$^2$ and LPM are calibrated for intensity. The precipitation accumulation of the PWD22 and Parsivel$^2$ are close to that of the gauge. The FD12P and LPM reports more and the PWS100 reports less accumulated precipitation. The VPF750 and particularly the SWS250 give a large underestimation of the accumulated precipitation. The distribution of the differences is narrowest for the PWD22, followed by LPM and PWS100, and the FD12P. The distribution is broadest for the VPF750, SWS250 and Parsivel$^2$. For light precipitation intensities the POD and FAR for PWD22 and FD12P are best and the POD is worst for PWS100. The LPM has the best scores for medium precipitation intensities. Large differences between the precipitation intensity reported by the PWS and the gauge occur for all PWS. The precipitation intensity of the LPM agrees, within the WMO uncertainty limits of ±0.1 mm/h or ±5 %, with the gauge about 60 % of the time. For the SWS250 agreement is reached 31 % of the time. For other PWSs the agreement with the gauge is between 38 and 45 %.

The MOR of the PWSs is compared to the reference MOR obtained by a transmissometer, which is only valid up to 2 km. The MOR reported by the PWS100 is too low over its entire MOR range. The MOR of the PWD22, VPF750 and SWS250 compare equally well with the TMM for fog. The FD12P has a slightly better POD, but the FAR is much worse due to a bias. For MOR between 800 and 1500 m the FD12P and PWD22 agree better with the TMM than the VPF750 and SWS250. There is no reference for large MOR values. There are systematic differences between the MOR reported by the PWSs. The scatter between the MOR values is large due to the temporal variability of MOR. Limiting the MOR to 20 km gives the best agreement with the MOR of the FD12P, within the WMO uncertainty limits, for the PWD22 (86 %). For the VPF750 and SWS250 agreement is reached 78 % and 79 % of the time. The agreement for MOR of the PWS100 is only 30 % due to the negative bias. Note that these scores are dominated by the cases with good visibility. The MOR reported by VPF750 and SWS250 sometimes show spikes with reduced MOR values during clear days while the TMM and other PWSs show no features in the MOR. The MOR obtained by all forward scatter sensors can be reduced when flying insects pass the measurement volume. The TMM is generally not affected by flying insects. The insect events occur during calm days in summer/autumn around sunset.

The results for the temperature of the PWSs are generally as could be expected from the location of the temperature sensor. The VPF750 and PWS100 use a separate temperature sensor in a radiation screen and agree best with the temperature of the AWS. The LPM has an external temperature sensor directly underneath the PWS and is third best. The PWD22 and SWS250, with the temperature sensor built into the PWS, have the worst agreement with the AWS. The temperature of all PWSs, except SWS250, is on average higher than that of the AWS. The VPF750 and PWS100 agree, within the WMO uncertainty limits of ±1 °C, with the AWS temperature about 99 % of the time. For the LPM1 and PWD22 agreement is reached 71 % and 68 % of the time, respectively. The agreement for temperature of the SWS250 and LPM2 is only 27 and 42 % due to the negative and positive bias, respectively. The best overall agreement of the temperature does not necessarily mean that the scores for the class temperature below zero is also the best. Also note that the temperature of any PWS can deviate several degrees from the AWS temperature at certain moments.

The field evaluation of the PWSs has not yet completed. The field test is ongoing and will include the next winter season of 2016/2017. The analysis of the data also requires further refinement. Therefore, no preferred PWS, considering the specific requirements and conditions in the Netherlands, has been identified at this moment. The preliminary results will be shared with the manufacturers and their feedback and/or optimizations will be taken into account. The results so far indicate that some problems KNMI experiences with the FD12P might be mitigated by other PWSs, but some new issues arise for specific sensors. At this moment no PWS seems to be able to solve all shortcomings of the FD12P while introducing no new issues. We take this opportunity to close with three more general observations:

1. Sensors should provide access to raw data of the physical quantities that are observed so that these quantities can be validated. It should be possible (by the manufacturer) to reprocess the raw data in order to optimize the sensor output.
2. PWSs should not only provide its best evaluation of the precipitation type, but it should also give information on the probability that each type could have occurred. This is essential quality information for the user. It also allows the user to further improve the precipitation type information using the output of the PWS in combination with information from other sources.
3. The MOR obtained by forward scatter sensors can be reduced by insects flying through the measurement volume. The MOR obtained by transmissometers is generally not affected by flying insects due to the larger measurement volume. Users; be aware that this problem can occur at locations / conditions favourable to flying insects. Manufacturers; please investigate whether the MOR reported by your forward scatter sensor is affected by flying insects and try to overcome this. As far as we know the FD12P was the only PWS that has firmware (1.92S) to filter out the spikes in the scattered signal due to flying insects (but not precipitation) before calculating the MOR. Obviously observations 1 and 2 facilitate handling this issue.

## REFERENCES

Bloemink, H.I., 2006: KNMI visibility standard for calibration of scatterometers, WMO Technical Conference on Instruments and Methods of Observations, 4 - 6 December 2006, Geneva, Switzerland.

De Haij, M. and W. Wauben, 2010: Investigations into the Enhancement of Automated Precipitation Type Observations at KNMI, WMO Technical Conference on Instruments and Methods of Observations, 30 August - 1 September 2010, Helsinki, Finland.

Leroy, M., and C. Bellevaux, 1998: PREWIC; The WMO intercomparison on present weather sensors/systems (Canada and France, 1993-1995). Final report. WMO, Geneva, Switzerland, IOM 73 (TD887).

Wauben, W.M.F., 2002: Automation of visual observations at KNMI: (i) Comparison of present weather, American Meteorological Society Symposium, 13-17 January 2002, Orlando, Florida.

Wauben, W.M.F., 2012: Filtering of insect reduced MOR measurements by a forward scatter sensor, WMO Technical Conference on Instruments and Methods of Observations, 6-18 October 2012, Brussels, Belgium.

Wauben, W.M.F., 2014: Unidentified Precipitation in Aeronautical Reports, Draft KNMI Technical Report, August 25, 2014, De Bilt, The Netherlands.